

SNOWFLAKES FALLING ON WATER:
THE UNDERWATER SOUND GENERATED BY
FALLING SNOW

TAHANI ALSARAYREH



Library and
Archives Canada

Published Heritage
Branch

395 Wellington Street
Ottawa ON K1A 0N4
Canada

Bibliothèque et
Archives Canada

Direction du
Patrimoine de l'édition

395, rue Wellington
Ottawa ON K1A 0N4
Canada

Your file *Votre référence*
ISBN: 978-0-494-41980-9
Our file *Notre référence*
ISBN: 978-0-494-41980-9

NOTICE:

The author has granted a non-exclusive license allowing Library and Archives Canada to reproduce, publish, archive, preserve, conserve, communicate to the public by telecommunication or on the Internet, loan, distribute and sell theses worldwide, for commercial or non-commercial purposes, in microform, paper, electronic and/or any other formats.

The author retains copyright ownership and moral rights in this thesis. Neither the thesis nor substantial extracts from it may be printed or otherwise reproduced without the author's permission.

AVIS:

L'auteur a accordé une licence non exclusive permettant à la Bibliothèque et Archives Canada de reproduire, publier, archiver, sauvegarder, conserver, transmettre au public par télécommunication ou par l'Internet, prêter, distribuer et vendre des thèses partout dans le monde, à des fins commerciales ou autres, sur support microforme, papier, électronique et/ou autres formats.

L'auteur conserve la propriété du droit d'auteur et des droits moraux qui protègent cette thèse. Ni la thèse ni des extraits substantiels de celle-ci ne doivent être imprimés ou autrement reproduits sans son autorisation.

In compliance with the Canadian Privacy Act some supporting forms may have been removed from this thesis.

Conformément à la loi canadienne sur la protection de la vie privée, quelques formulaires secondaires ont été enlevés de cette thèse.

While these forms may be included in the document page count, their removal does not represent any loss of content from the thesis.

Bien que ces formulaires aient inclus dans la pagination, il n'y aura aucun contenu manquant.


Canada

**Snowflakes Falling on Water: the Underwater Sound
Generated by Falling Snow**

by

© Tahani Alsarayreh

A thesis submitted to the
School of Graduate Studies
in partial fulfillment of the
requirements for the degree of
Master of Science.

Department of Physics and Physical Oceanography
Memorial University of Newfoundland

ST. JOHN'S

NEWFOUNDLAND

Contents

Abstract	iv
Acknowledgements	v
List of Tables	vi
List of Figures	vii
1 Introduction	1
1.1 Motivation	1
1.2 Literature review	3
1.3 Snow classification	15
1.3.1 The snow classification systems	15
1.4 Objectives	21
1.5 Outline	22
2 Instrumentation and methods	23
2.1 Instrumentation	24
2.2 Data processing	29

2.2.1	Instruments calibration	29
2.3	General method	31
3	The Results and Discussion	37
3.1	The Results	37
3.1.1	Spectra for different snowfall types	37
3.1.2	A comparison between rain and snow spectra ..	41
3.1.3	The relationship between sound level and snowfall rate	44
3.1.4	Wind speed effect at frequencies below 4 kHz ..	47
3.1.5	Snow spectra at frequencies between 10 – 15 kHz	49
3.1.6	Snow spectra at frequencies above 30 kHz	51
3.2	Discussion	55
3.2.1	Different snowflake types produce different snow spectra	55
3.2.2	Snowfall rate measurements	59
4	Summary and Conclusions	61
4.1	Future work	64
	Bibliography	66
	Appendix A	71

Abstract

There have been a few reports that snow generates sound similar to that of rain when it strikes the ocean surface but it is hard to imagine that the mechanisms responsible for rain sounds could be the same as those that cause sound from falling snow. We explore the sound generated by falling snow through laboratory measurements under different atmospheric conditions that give rise to variety of snowflake types with different snowfall rates by using a small tank filled with tap water. We find that there is a well defined spectral peak at around 12 kHz (similar to that of rain) in sound generated by some snow types; other snow types do not produce appreciable underwater sound. The data suggest that the sound generated by falling snow is such that ocean snowfall rates could be estimated by evaluating spectral characteristics of the sound. More experiments need to be done for that purpose as sound levels depend on snowfall rate, snow types, sea state, and wind speed.

Acknowledgements

First I would like to thank my husband, Hassan, for his support and help through the whole process. And thanks to my mother and father, have always helped me by their prayer and encouragement.

I would like to express my deep gratitude to Dr. Len Zedel for his supervision, guidance and patience. I would like also to thank him for providing support and a great learning environment.

Thanks also to Chris Stevenson for the continuous computer support and assistance. Thanks to Jack Foley for his technical support.

The financial support from the Department of Physics and Physical oceanography, the School of Graduate Studies, Memorial University of Newfoundland and my supervisor Len Zedel were greatly appreciated.

List of Tables

2.1 The resonance frequency of the tank	27
---	----

List of Figures

1.1	Underwater sound spectra generated by hail	5
1.2	Underwater sound generated by wind and rain	7
1.3	Underwater sound generated by snow	11
1.4	Underwater signature generated by snow	13
1.5	Underwater acoustic emissions for a raindrop and a snowflake as they strike the water surface	14
1.6	The international snow classification scheme	17
1.7	The Magono and Lee classification scheme	18
1.8	A photograph for the detected snow crystal types	20
1.9	A photograph for Graupel snow type	21
2.1	The tank used in the experiment	25
2.2	Raw data receiving response for the hydrophone	30
2.3	A diagram shows the experiment setting	33
2.4	The sound spectrum generated by snow	34
2.5	The spectra of the background noise	36
3.1	The spectra of the seven detected snow types	39
3.2	The spectra for Spatial dendrite and Plate flakes with the background noise	42
3.3	The spectra of the resonant flakes and light rain	43
3.4	The power spectral density for different snow events and different snowfall rate.....	45
3.5	The averaged spectral level of frequencies below 4 kHz as a function of wind speed	48
3.6	The averaged spectral level of frequencies between 10 – 15 kHz with respect to snowfall rate	52
3.7	The averaged spectrum level of frequencies above 30 kHz as a function of snowfall rate.....	54
3.8	A comparison between rain gauge data and radar data	60

Chapter 1

Introduction

1.1 Motivation

For several decades, oceanographers have given much consideration to ocean ambient sound, but mostly from the perspective of a noise source for acoustic systems. Many sources are responsible for underwater sound which can be categorized into three major categories; water motion including breaking waves, precipitation; manmade sources, and biological sources (Wenz, 1962). Only over the last twenty years have oceanographers and meteorologists given special attention to underwater sound generated by precipitation (rain, hail, and snow), and wave breaking as a signal in itself of interest. Rather than simply contributing to a background noise spectrum it has been realized that these acoustic sources can provide information on the underlying source processes (i.e. rain, snow, and wind).

Precise measurements of rainfall, snow and hail are necessary in understanding climatic processes in both regional and global scale. In addition, knowing the characteristic acoustic signature for each type of source is needed to better predict the performance of all acoustical instruments in the presence of “noise”. Direct measurements of rainfall rate at sea is very complicated due to the difficulty associated with instrument deployment in the ocean including biological fouling, platform stability, and exposure to extreme weather (waves) (Nystuen and Selsor, 1996). In this hostile environment, rain gauges give inaccurate measurements of rainfall rate over oceanic regions. Fortunately, underwater sound generated by rain can be used to quantitatively measure the rainfall rate (Nystuen, 1985). Snow has been given less attention than other types of precipitation, but some observations recognized it as a distinct sound source (Scrimger et al., 1986).

In addition to filling a clear gap in ocean noise data the motivation for our study on snow in particular is curiosity; it’s easy to believe that rain and hail produce sound when they strike the water, but not for snow; because of the smaller momentum that is transferred into the water as a result of the impact. Snow falls in different shapes, sizes and under a variety of weather

conditions. It's necessary to discriminate between snow types that can make sound and others that can't. This is a distinction that has not been previously attempted as for the other types of precipitation, it's important to characterize the snow signal for every snow type. Measuring snow falling rate into the ocean is difficult for the same reasons discussed above as in the case of rain. And data taken from sensors and gauges used to measure snow fall rate are not accurate because some snow types can't be detected by these sensors. Acquiring accurate acoustic spectra for each snow type will contribute to an ability to estimate snowfall rate using underwater sound.

1.2 Literature review

Underwater noise spectrum levels were first characterized by Knudsen (1948) for frequencies between 100 Hz – 25 kHz. The spectrum levels depend on wind speed, and spectrum levels decrease as the frequency increases (Medwin and Beaky, 1989). Wenz (1962) speculated that air bubbles produced near the sea's surface due to wind could be the major source for wind dependent ambient noise. The air bubble source of wind generated sound has been demonstrated to be the case as shown in studies by Melville et al. (1988).

Breaking waves (Farmer and Vagle 1988) generate the main source of the ambient sound, which is affected by wind speed. The importance of estimating oceanic winds by measuring the wind generated ambient sound arises as a result of the lack of the availability of accurate wind speed measurements at sea. Vagle et al. (1990) established a WOTAN (Weather Observations through Ambient Noise) wind algorithm relating sound spectrum level to wind speed (for winds less than 16 m/s).

A strong sound generation would be expected for solid precipitation in the form of hail because of the large impact and consequent energy transfer to the water. Scrimger et al. (1987) observed hail generated sound in a small lake; Figure (1.1) shows underwater noise spectra produced by hail at different wind speeds. The hail spectra have a characteristic peak at frequency ranges between 2.3 – 5 kHz and the peak width is independent of wind speed.

Rain as an underwater sound source was recognized very early on Knudsen et al. (1948), but there was no clear relationship between sound level and rainfall rate. This situation was a result of the complicated nature of rain generated sound and its dependence on raindrop size, rainfall rate and

wind speed. For sound spectra generated by light rain the signal is complicated, as

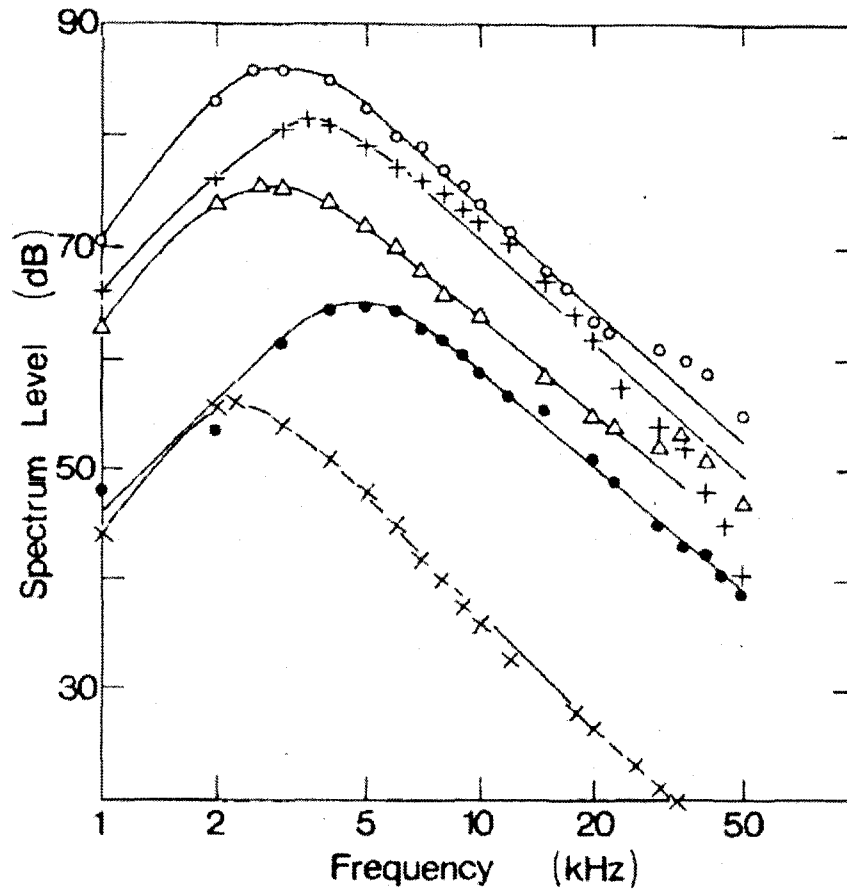


Figure 1.1. Five examples of underwater sound spectra generated by hail in different wind speed conditions (taken from Scrimger et al., 1987). The spectral levels measured in dB as a function of frequency in kHz. The observed hail spectra correspond to wind speed and the frequency where the peak appears respectively is; (o) 1.8 m/s 2.9 kHz, (+) 2.7 m/s 3.9 kHz, (Δ) 2.7 m/s 2.9 kHz, (\bullet) 1.4 m/s 5kHz, (\times) 3.4 m/s 2.3 kHz.

they are wind speed sensitive. When such rain is accompanied with light wind speed (<1.2 m/s), rain spectra will have a characteristic peak at about 13.5 – 15 kHz. Figure (1.2) represents wind spectra for different wind speed, and the rain spectra for light and heavy rain. As the wind speed increases the spectral peak becomes more rounded (Scrimger et al., 1987). Light rain or drizzle contains small raindrops that generate sound with a peak at around 15 kHz, which is poorly correlated to rainfall rate (Nystuen et al., 1993). At higher wind speeds this spectral peak disappears because the raindrops no longer entrain air bubbles as they strike the water.

In contrast, for large raindrops that typically occur during periods of heavy rainfall, the sound generated is caused by the direct impact of the rain on the water surface. This sound is not strongly dependent on wind speed and provides a sound level that correlates well with rainfall rate (Nystuen, 1986, Nystuen et al. 1993). Heavy rainfall has many large raindrops which smoothes the characteristic peak at 15 kHz (Nystuen et al., 1993). Nystuen et al. (1992) study the sound generated by individual raindrops with a whole

range of raindrop sizes at their terminal speed. The raindrops divided into four different sizes; minuscule drops (Diameter $D < 0.8$ mm), small

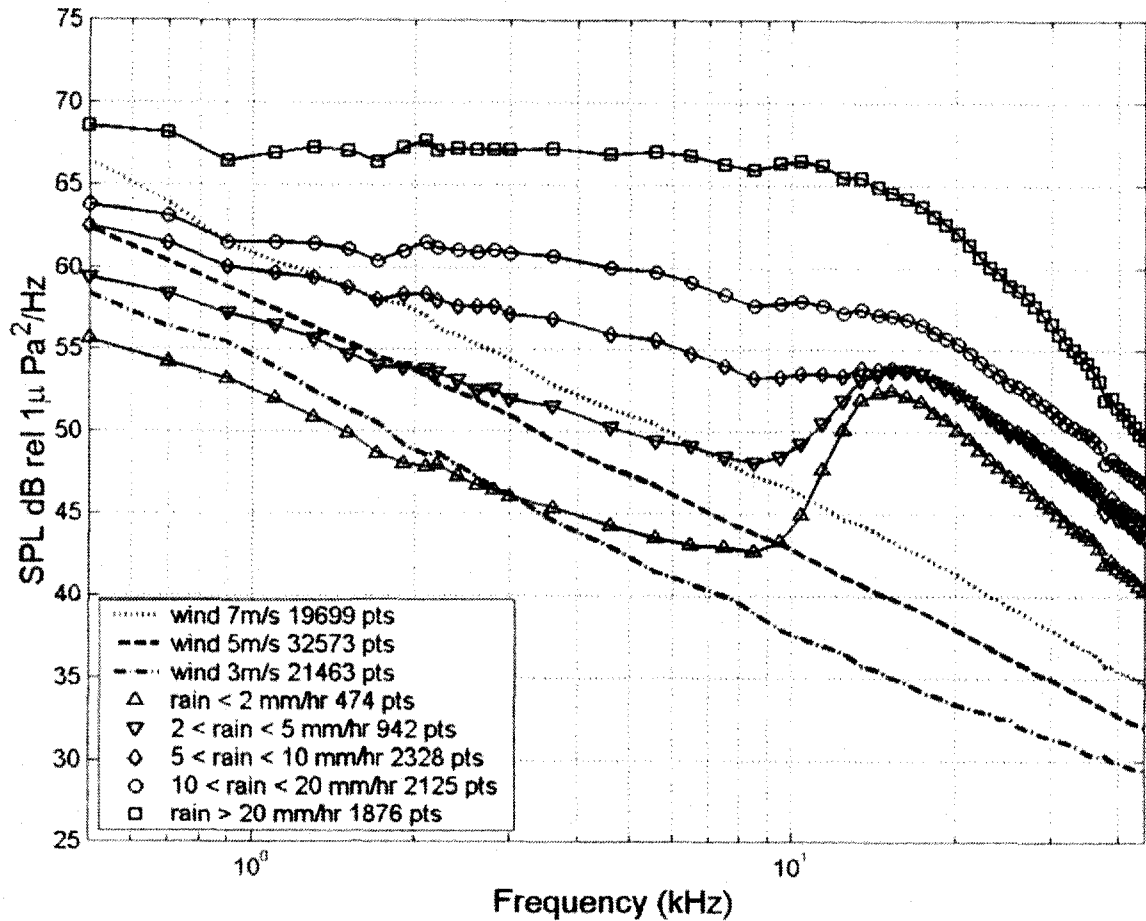


Figure 1.2. The underwater sound spectra generated by wind with different wind speed, and rain with different rainfall rate. (This Figure is taken from Ma and Nystuen 2005).

drops ($0.8 \text{ mm} \leq D \leq 1.1 \text{ mm}$), mid-size drops ($1.1 \leq D \leq 2.2 \text{ mm}$), and large drops ($D > 2.2 \text{ mm}$). They predicted the intensity spectral density levels from the knowledge of drop size distribution, and showed that there is a possibility to determine the rainfall rate from the predicted spectra. Nystuen (2001) had successfully applied an inversion algorithm method to determine rainfall rate for rain with different raindrop sizes, which are tiny, small, medium, large and very large raindrops. This method depends on the physics of underwater sound generated by these raindrops. As each raindrop size has different splash physics. For example; the tiny raindrop has a gentle splash nature that doesn't make sound, small raindrops have a gentle splash nature accompanied with bubble formation in every splash, the medium raindrop has gentle splash nature with no bubbles, and large and very large raindrops have turbulent irregular bubbles entrainment.

In contrast to the theoretically based algorithm developed by Nystuen (1996), another successful quantification for rainfall rate was done by Ma and Nystuen (2005). In order to get precise measurements of sound pressure level, they have applied a new calibration method based on the sound signal

generated by wind, assuming that the wind signal is universal. Then they used an empirical algorithm method applied to deep ocean sound levels by using a simple relationship between sound intensity and rainfall rate in the form

$$I = aR^b \quad (1.1)$$

where I is the sound intensity, R is the rainfall rate. Then taking the $10\log_{10}$ of equation (1.1) at one particular frequency which is 5 kHz, as the rain spectra at this frequency is wind independent. The result of this method is the equation

$$dBR / 10 = \frac{(SPL_{5kHz} - 42.4)}{15.4} \quad (1.2)$$

where $dBR = 10\log_{10}(R)$, SPL is the sound pressure level (dB relative to $1\mu\text{Pa}^2\text{Hz}^{-1}$) at 5 kHz, 42.4 represents the intercept, and 15.4 represents the spectral slope. Equation (1.2) is similar to the relation used by Nystuen (1996). This method allows calculating rainfall rate from sound pressure

level and gave a good agreement with rainfall measured by rain gauges and satellite data. Ma and Nystuen (2005) divided sound spectra for heavy rain, drizzle and wind into five sections, and empirically modeled their data to predict underwater sound levels from rain and wind using wind speed and rainfall rate as input data for frequency range from 1 – 50 kHz.

In contrast to the rich literature available on rain generated sound, very little has been reported on snow sounds. The first observation for underwater sound generated by snowfall was by Scrimger in (1985), when he noticed an increase of the background noise attributed to a snowing event. But he unfortunately didn't measure the complete frequency spectrum, just sound level at a few prescribed frequencies. Again Scrimger et al. (1987) measured sound spectra generated by snow in a fresh water lake including three snow events: figure (1.3) shows these three spectra measured at different snowfall rate. The spectra have 2 to 3 dB differences in spectral levels between events and they appear as a linear rise in sound levels between 36 – 40 dB with 5 dB/oct spectral slope at frequency above 35 kHz. He described the snow events as calm with low wind speed and large gently falling flakes (Scrimger et al. 1987). There was no quantitative data obtained about snowfall rate, water temperature, or snow type.

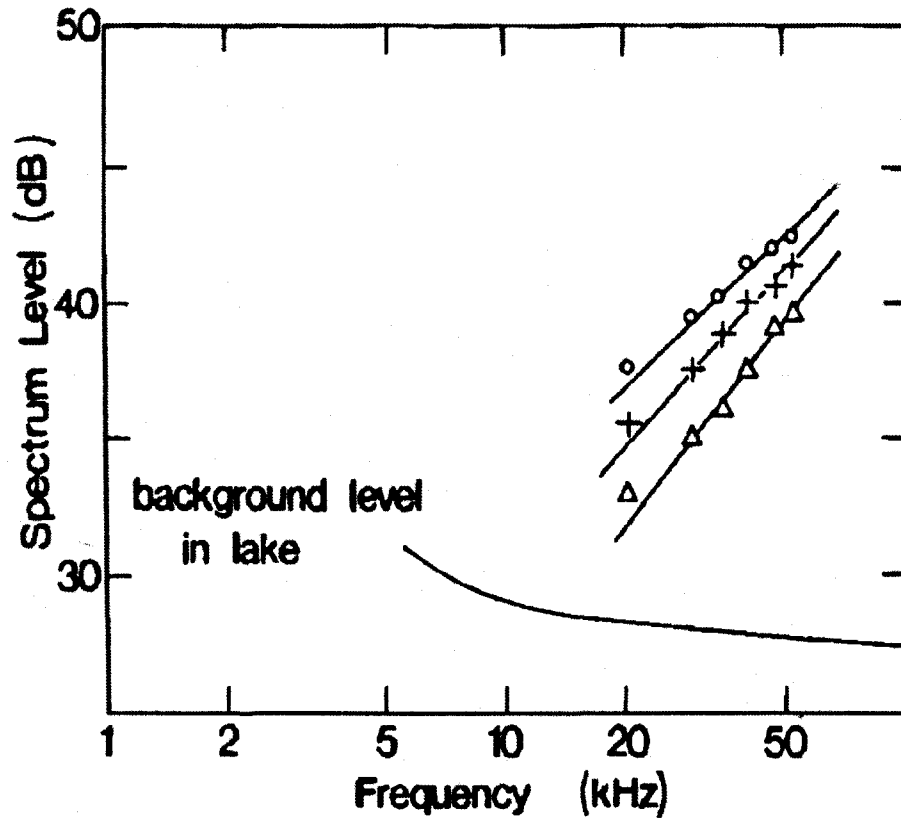


Figure 1.3. Underwater sound spectra generated by three different snow events. (This figure is taken from Scrimger et al. 1987).

Another measurement for underwater sound generated by snow was from Behm Canal, Alaska (McConnell et al., 1992). The snow spectra showed an increase in spectral levels above 40 kHz for all snow events recorded including heavy snowfall rate with light wind speed as shown in Figure 1.4. The vertical lines represent the spectra given by Scrimger et al. (1987) and show a similarity to the spectra from Alaska. Also there was no increase in sound level measured below 10 kHz (McConnell et al., 1992). Crum et al. (1999) studied the acoustic signal produced from the impact of individual snowflakes on water in a small container. Also he compared the pressure time traces between raindrop and snowflake impacts, the raindrop contains two parts; the first small bump is associated with the direct impact of the rain drop with water as seen in Figure (1.5). The second bump is a decaying sinusoid due to a gas bubble entrained into the water as a result of the impact. The underwater acoustic emission for the snowflake shows an initial growth for the signal then a slow decay as of a resonant source. Both traces have nearly the same decay constant which equals the expected decay constant for freely oscillating bubbles; this indicates that underwater signature produced by snow and rain are in this example both due to oscillating gas bubbles.

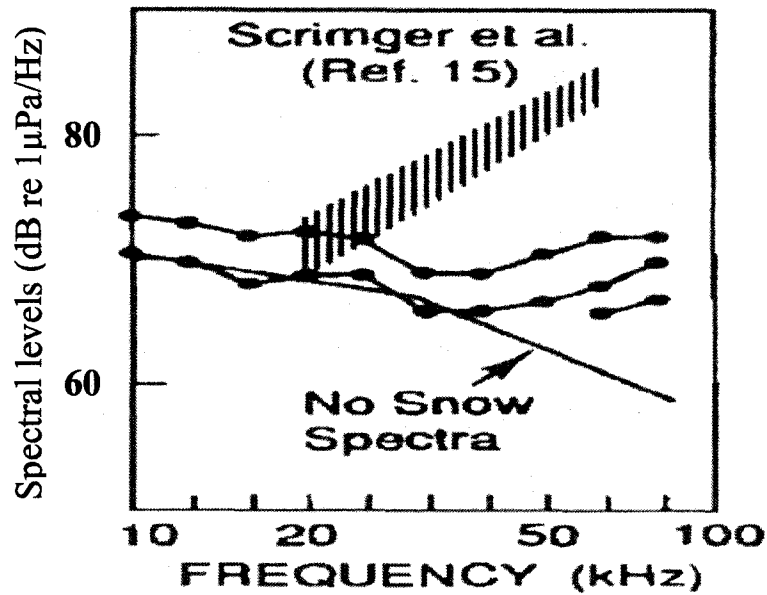


Figure 1.4. Underwater signature generated by snow. The spectra appear as a gradual rise in spectral levels above 40 kHz. The vertical lines represent the snow spectra by Scrimger et al. (1987), the solid line represents the spectra without snow. The spectral levels are in dB (re 1 μ Pa/Hz) and the frequency in kHz. (This Figure is taken from McConnell et al. 1992).

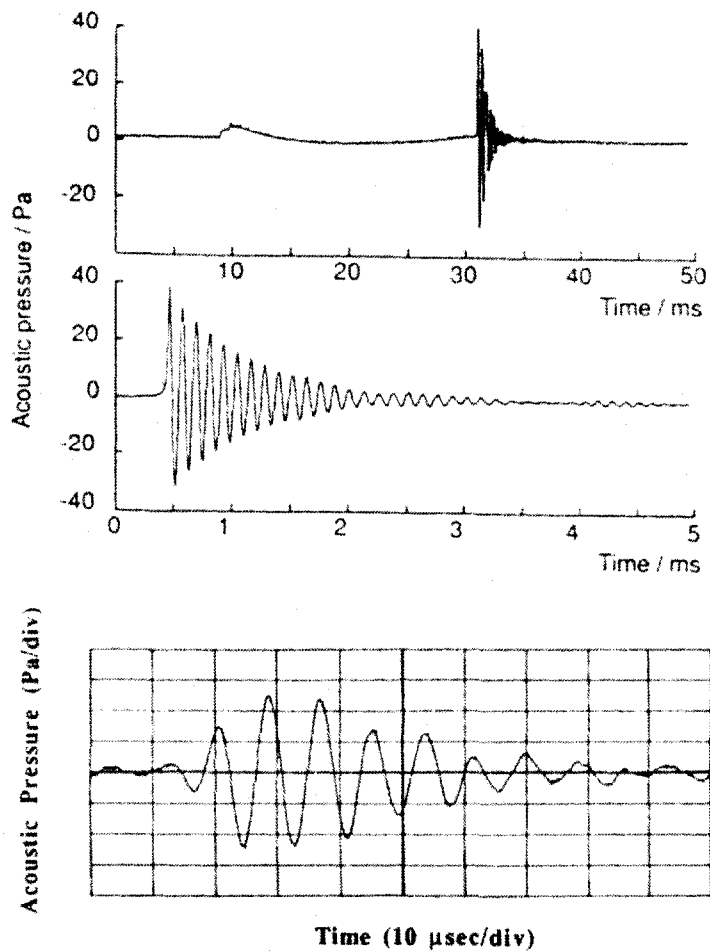


Figure 1.5. Underwater acoustic emissions for a raindrop and a snowflake as they strike the water surface. The above graph shows the impact signal and the decaying sinusoid due to gas bubble entrainment to water which is shown in more detailed in the middle graph. The bottom graph shows the acoustic emission for a snowflake impact (This Figure is taken from Crum et al. 1999).

1.3 Snow classification

Ice crystals (snow crystals) come in many forms ranging from well formed six sided ice crystals to large random accumulations of small ice crystals. These different ice crystals arise because of temperature, humidity and the time history of the ice crystals growth. Ice crystals are formed as a result of accumulation of ice particles around ice nuclei which could be dust particles or tiny crystals of sea salt, these ice particles are formed in clouds (LaChapelle, 1969). Aggregations of ice crystals are called snowflakes. When there is enough humidity and temperatures are below freezing, ice particles continue growing to form ice crystals. These may aggregate to form snowflakes. In time, the crystal size increases enough so that the ice crystals or snowflakes fall to the ground as solid precipitation (Hobbs, 1974). Our concern is snow crystal type, which we will talk about in the next section.

1.3.1 The snow classification systems

One of the common snow classification systems was proposed in 1951 by the Commission of Snow and Ice of the International Association of Hydrology, this classification divides snow types into ten classes as

presented in Figure (1.6). This Figure shows general shapes for each type of snow crystal; Plate, Stellar crystal, Column, Needle, Spatial dendrite, Capped column, Irregular crystal, Graupel, Ice pellet, and Hail (Hobbs, 1974). A much more detailed classification was developed by Nakaya using the method of photomicrography (Nakaya, 1954). Nakaya's classification scheme was modified by Magono and Lee in (1966) as shown in Figure (1.7); it holds about 99 per cent of the observed snow crystals (LaChapelle, 1969). Although the Magono and Lee classification scheme is much more detailed than the international classification scheme, we used the International Classification system to classify snow crystals in the experiments. The international system is simpler, and can fit most of the snow types observed during the experiments. In addition, in this study it is not necessary to classify beyond the international classification scheme because each type would have the same mechanisms in generating underwater sound signature. For example we need only to classify Plate crystal from other types of snow crystals rather than classify Plate into many types as Magono and Lee do in their classification system. During this study seven snow types were observed; Plate, Stellar crystal, Column, Needle, Spatial dendrite, Irregular crystal and Graupel. The following discussion

Produce Acoustic sound . Type of particle

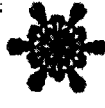
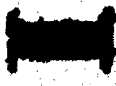
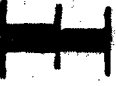
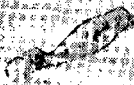
	TERM	TYPICAL FORMS		
No	PLATE			
No	STELLAR CRYSTAL			
Yes	COLUMN			
Yes	NEEDLE			
No	SPATIAL DENDRITE			
NA	CAPPED COLUMN			
Yes	IRREGULAR CRYSTAL			
Yes	GRAUPEL			
NA	ICE PELLET			
NA	HAIL			

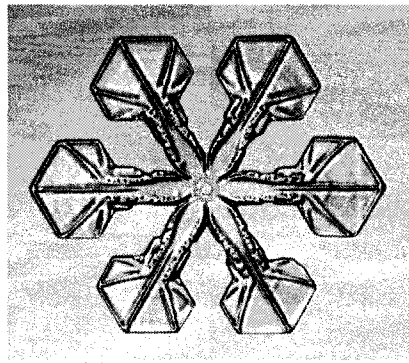
Figure 1.6. Snow classification scheme suggested by the Commission of Snow and Ice of the International Association of Hydrology. (This photo was taken from Hobbs, 1974). (Yes) acoustically noisy, (No) acoustically quiet and (NA) unobserved.

	N1a Elementary needle		C1f Hollow column		P2b Stellar crystal with sectorlike ends		P6b Plate with spatial dendrites		CP3 d Plate with scrolls at ends		R3c Graupelike snow with nonrimed extensions
	N1b Bundle of elementary needles		C1g Solid thick plate		P2c Dendritic crystal with plates at ends		P6c Stellar crystal with spatial plates		S1 Side planes		R4a Hexagonal graupel
	N1c Elementary sheath		C1h Thick plate of skelton form		P2d Dendritic crystal with sectorlike ends		P6d Stellar crystal with spatial dendrites		S ₂ Scalelike side planes		R4b Lump graupel
	N1d Bundle of elementary sheaths		C1i Scroll		P2e Plate with simple extensions		P7a Radiating assemblage of plates		S3 Combination of side planes, bullets and columns		R4c Conelike graupel
	N1e Long solid column		C2a Combination of bullets		P2f Plate with sectorlike extensions		P7b Radiating assemblage of dendrites		R1a Rimmed needle crystal		I1 Ice particle
	N2a Combination of needles		C2b Combination of columns		P2g Plate with dendritic extensions		CP1a Column with plates		R1b Rimmed columnar crystal		I2 Rimmed particle
	N2b Combination of sheaths		P1a Hexagonal plate		P3a Two-branched crystal		CP1b Column with dendrites		R1c Rimmed plate or sector		I3a Broken branch
	N2c Combination of long solid columns		P1b Crystal with sectorlike branches		P3b Three-branched crystal		CP1c Multiple capped column		R1d Rimmed stellar crystal		I3b Rimmed broken branch
	C1a Pyramid		P1c Crystal with broad branches		P3c Four-branched crystal		CP2a Bullet with plates		R2a Densely rimmed plate or sector		I4 Miscellaneous
	C1b Cup		P1d Stellar crystal		P4a Broad branch crystal with 12 branches		CP2b Bullet with dendrites		R2b Densely rimmed stellar crystal		G1 Minute column
	C1c Solid bullet		P1e Ordinary dendritic crystal		P4b Dendritic crystal with 12 branches		CP3a Stellar crystal with needles		R2c Stellar crystal with rimmed spatial branches		G2 Germ of skeleton form
	C1d Hollow bullet		P1f Fernlike crystal		P5 Malformed crystal		CP3b Stellar crystal with columns		R3a Graupelike snow of hexagonal type		G3 Minute hexagonal plate
	C1e Solid column		P2a Stellar crystal with plates at ends		P6a Plate with spatial plates		CP3c Stellar crystal with scrolls at ends		R3b Graupelike snow of lump type		G5 Minute assemblage of plates
											G6 Irregular germ

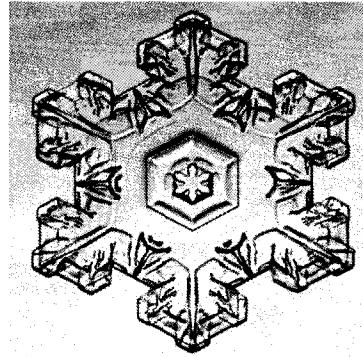
Figure 1.7. The meteorological classification system of snow crystals modified by Magono and Lee (1966).

gives a brief description of each of the observed types detected in the experiments. This description was taken from the international classification scheme (Hobbs, 1974).

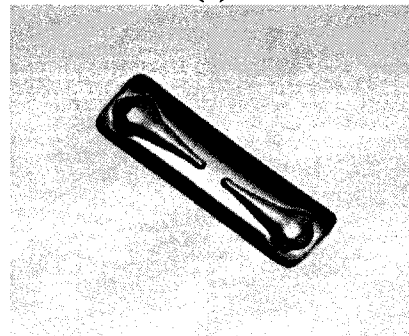
1. Plate is usually a hexagonal thin plate, have edges with similarity in length and pattern as seen in Figure (1.8, a).
2. Stellar crystal is a thin flat snow crystal like a star with three, twelve, or six arms formed in one plane or more as shown in Figure (1.8, b).
3. Column is a prismatic crystal, which could be solid, or hollow, the ends of Column could be plane, pyramidal truncated or hollow as in Figure (1.8, c).
4. Needle is a very slim cylindrical crystal shown in Figure (1.8, d).
5. Spatial dendrite is a large snow crystal with fern like arms which lie in many different planes as in Figure (1.8, e).
6. Irregular crystal is a snow crystal containing of many small crystals grown in arbitrary manner as seen in Figure (1.8, f).
7. Graupel is a snow crystal that is coated heavily with frozen rain drops called rime shown in Figure (1.9).



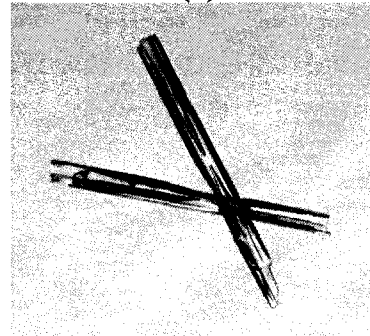
(a)



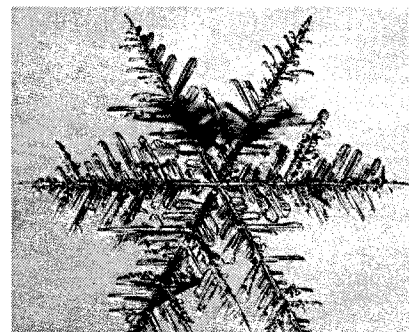
(b)



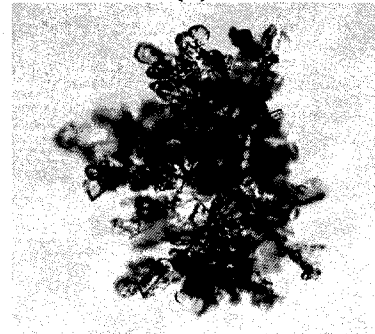
(c)



(d)



(e)



(f)

Figure 1.8. A photograph for the snow crystal detected through the experiments. The graph was taken from the web site (<http://www.agiudetosnowflake>). The snow crystals are (a) Plate, (b) Stellar, (c) Column, (d) Needles, (e) Spatial dendrite, (f) Irregular.

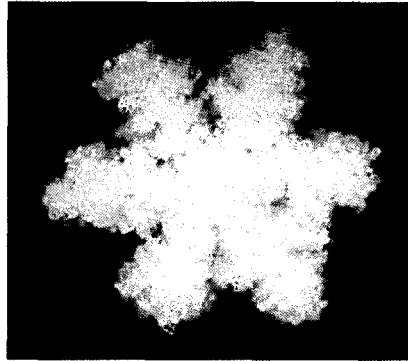


Figure 1.9. A photograph for snow crystal of Graupel type. Taken from the web site (<http://www.agiudetosnowflake>).

1.4 Objectives

Surprisingly, the relation between the snowfall rate and spectral levels had never been studied before. The limited studies on this topic only mention underwater sound produced by snow (Crum et al. 1999, McConnell et al. 1992, Scrimger et al. 1987). The only thing that is mentioned about the snow spectra from the previous studies is that snow spectra appear as a gradual increase in spectral levels above a frequency of about 40 kHz (Scrimger et al. 1987). And none of these studies described the snow type. This study will give a better understanding of the underwater sound spectra

made by snow and give an idea of the relation between spectral levels and snowfall rate. The objectives of this study are as follows:

- To identify which of the snowflake types create a characteristic sound.
- Determine the characteristic sound spectrum for each snow type that makes underwater sound.
- Compare the difference between the snow spectra and light rain spectrum.
- To explore the relation between sound level and snowfall rate.

1.5 Outline

The remainder of this thesis will be arranged as follows: in chapter 2, a brief description of the instruments used in the experiment and the settings is given and the methodology of the work is discussed. In chapter 3, the results of the work are presented and discussed. In chapter 4, the work done in the thesis is summarized and some suggestions for future work are given.

Chapter 2

Instrumentation and methods

The instrumentation required to record underwater sound is similar to that used for typical in-air sound recording. The special considerations for the present study are that snowflakes must strike the water surface and frequencies in the range 10 – 50 kHz must be recorded consistent with the observations of Crum et al. (1999). The method used has been to follow the approach of Crum et al. (1999) using a small tank to measure the signal as snow was falling. These experiments were held in St. John's, Newfoundland a familiar place for snow storms and cold weather. Fourteen experiments were undertaken outside the Physics-Chemistry building, on the Memorial University Campus during different snowfall situations and different snow rates, in the winter 2007 from February 2 – April 3. Another experiment was made to measure the sound of rainfall for comparison purposes.

The aim of these experiments was; to record the underwater sound signature generated by different snow types, determine which types make a characteristic underwater sound, to compare between rain and snow spectra, and to explore the relation between snowfall rate and sound level. The Instrumentation used in the experiments are discussed in section 2.1, then a general description of the overall experiment is discussed in section 2.2.

2.1 Instrumentation

A tank with dimensions $80 \times 60 \times 60$ cm, covered on the outside with insulating material preventing temperature loss during the experiments is shown in Figure (2.1). The tank was filled with approximately 47-cm depth of tap water. Mounted on wheels, the tank was pulled outside whenever snow was falling then pulled inside the building so the water in the tank would not freeze during the night.

In a small tank, natural resonance frequencies can affect any sounds that are generated in the tank. In order to know the frequency range that is affected by the resonance frequency of the tank, we calculate the resonance frequency using the following relation



Figure 2.1. The tank used in the experiments with dimension $80 \times 60 \times 60$ cm filled with tap water and a hydrophone replaced in the middle at 14 cm below the water surface.

$$f = c / \lambda, \quad (2.1)$$

Where c is the sound speed in water 1482 m / sec, λ is the wavelength.

$$\lambda = 2L, \quad (2.2)$$

and L is the tank dimension. The frequency of the fundamental mode is

$$f = c/2L. \quad (2.3)$$

We assume the tank has pressure release surfaces on all sides (as in the classic open cylinder problem), and it can produce all harmonics so

$$f = n \left(\frac{c}{2L} \right), \quad n = 1, 2, 3, \dots \quad (2.4)$$

Table (2.1) shows the resonance frequency for all tank dimensions; length, width, and water height for the first three modes.

As we can see from the table, the resonance frequency contributes the generated sound in the range between 1 – 4.7 kHz assuming high order

resonances are harder to excite. The resonance frequency of the tank is much lower than the high frequency sound expected for snow. Even if these resonances extend to higher modes, the frequency separation of about 1 kHz will not overly distort the high frequency signals of interest in the present study.

Table 2.1. The resonance frequency in kHz for the tank

Mode (kHz)	Length (L = 0.8m)	Width (W = 0.6m)	Height (H = 0.47m)
f_1	0.926	1.24	1.58
f_2	1.853	2.47	3.15
f_3	2.779	3.71	4.73

An ITC – 6050C hydrophone manufactured by the International Transducer Corporation was located in the middle of the tank 14 cm below the water surface. The hydrophone signals were amplified with a Reson VP2000 Voltage Preamplifier with 500 Hz high pass and 50 kHz low pass filter settings and 10 dB of gain.

A Personal Daq / 3000 series manufactured by IOtech, Inc. was used to digitize output from the Preamplifier. The Personal Daq / 3000 series makes digital samples with 16-bit resolution at a sample rate of 1-MHz and allows the viewing and storage of data using Matlab™ programs. The DAQ 3000 was factory calibrated via a digital NIST (National Institute of Standards and Technology federal agency) traceable calibration method. This calibration works by storing a correction factor which is calculated by the factory for each range on the unit at the time of calibration.

Snowfall observations were made using an Optical Scientific, Inc. OWI-430 DSP-WIVIS™ sensor mounted on the roof of the Chemistry – Physics building. This instrument optically measures the rate of falling rain, snow, drizzle, freezing and mixed precipitation conditions.

Because temperatures were not cold enough during the experiments (between 0 and -5°C) to preserve snow crystals from melting or losing their shape; it was necessary to observe snow crystal types immediately after they fell on a dark cloth. A hand lens was used to classify snow types visually using the International snow classification described in chapter one.

2.2 Data processing

2.2.1 Instruments calibration

The ITC hydrophone converts acoustic pressure fluctuations into voltages that have been recorded. In order to calculate the pressure measured by the hydrophone from that recorded data we must use the hydrophone receiver response and the following relation (Medwin & Clay 1998)

$$P = \frac{V}{G \times K} \quad (2.5)$$

where P is the calculated pressure in μPa , V is the output voltage in Volts, G is the signal amplification (10 dB), and K is the gain sensitivity in $\text{V} / \mu\text{Pa}$.

Gain sensitivity of the transducer was calculated using the receiver voltage response ($TRVR$) as follows

$$TRVR = RI + \delta \quad (2.6)$$

Where RI is the reference line computed from the raw data receiving response in Figure (2.2) and equal to -166 dB, δ is the difference between

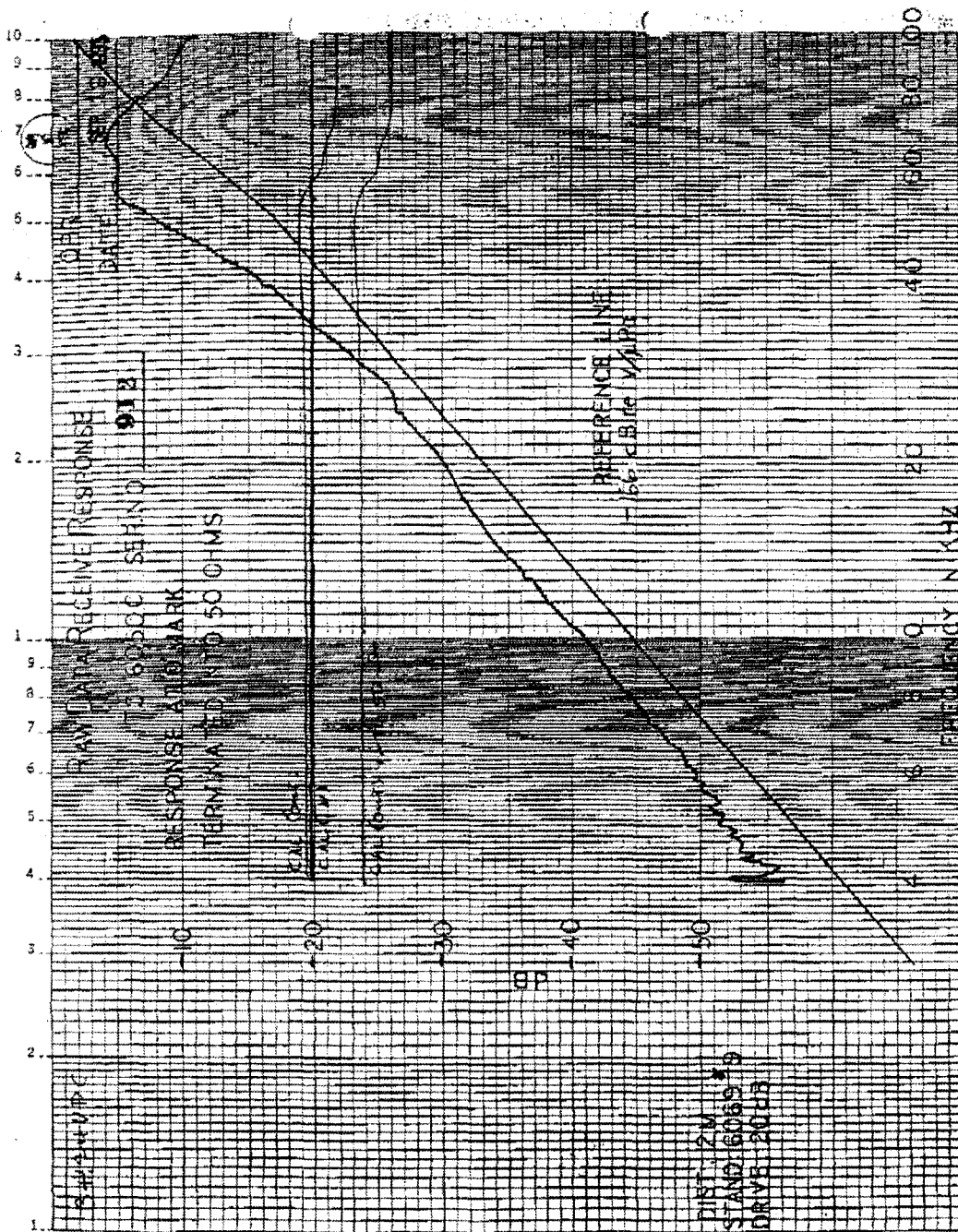


Figure 2.2. Raw data receiving response for the hydrophone in dB as a function of frequency (kHz), the graph shows the reference line -166 dB (re. 1 v/μPa) and the trace line.

the reference line and the plotted trace line, which is about 4 dB. Then the gain sensitivity can be calculated as

$$K = 10^{TRVR/20} = 7.9 \times 10^{-9} \text{ V} / \mu\text{Pa} \quad (2.7)$$

2.3 General method

In all experiments a general technique was used which will be described in the following section including the Matlab script used in analyzing the collected data. In each experiment the following data were recorded; time, water temperature ranging from 14.5°C to 7 °C, air temperature ranging from - 5°C to 0°C, hydrophone depth ranging from 13 to 14 cm. Also wind speed was measured using the roof – top weather station every 5 minutes then these values were averaged over the time of the experiment. Snow type was determined by eye and a hand lens. Snowfall rate was measured every minute by the OWI-430 gauge then averaged over the whole time of the experiment. Snowfall rates were also compared with the averaged snowfall rate over the same period measured by radar images from the Environment Canada web site

<http://www.weatheroffice.gc.ca/radar>. These radar images were recorded and saved every ten minutes.

The data was recorded for each snowfall event in several runs each of 5 seconds. The hydrophone signal was passed through the preamplifier to reduce aliasing then to the Personal Daq and finally converted into a Matlab file. Figure (2.3) shows a diagram for the experiment setting. A matlab script was used to analyze the data and create snow and rain spectra, this is done by converting data from voltage (V) to pressure (μPa) as described in section 2.1. The signal is then passed through a high – pass digital filter with cutoff frequency of 1000 Hz using butterworth function from MatlabTM filter design. Finally the power spectrum is calculated using the FFT and Pwelch functions in MatlabTM described in appendix A, and then taking the mean of all calculated spectra of the same event and converted it into decibel (dB). For studying the data with different snow types, the recorded data was first sorted by the type of snow and these data were all averaged together. For studying the relation between the sound levels and snowfall rate, data recorded was sorted by snowfall rate for each snow event, and then averaged over the whole time of the experiment.

Figure (2.4) represents one of the spectra calculated using the method described above. This spectrum collected during “periods” of heavy snowfall rate, which identifies three distinct spectral regions that will be

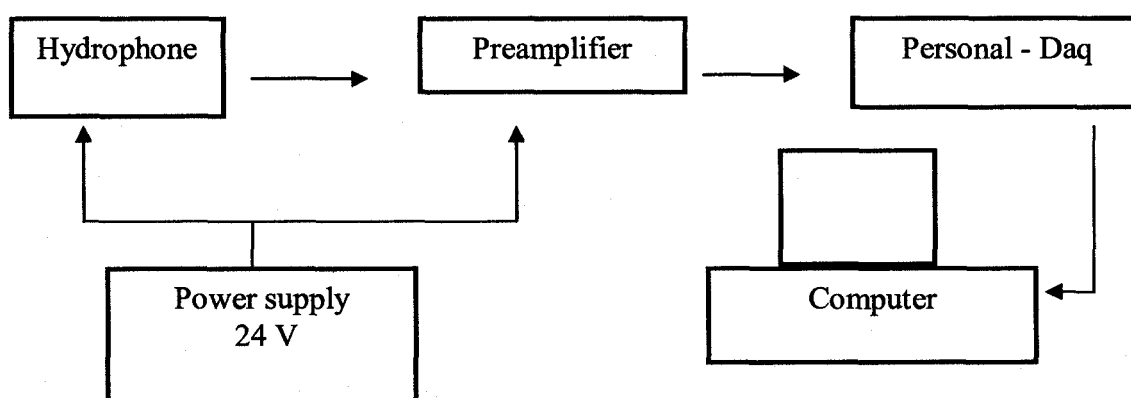


Figure 2.3. A diagram shows the experiment setting.

discussed in chapter 3. The high sound level that were often seen at frequencies below 4 kHz, the peak at about 12 kHz, and the gradual rise in spectral level above 30 kHz can be observed.

In order to calculate the background noise contributed with the recorded signal, data was collected during periods of no precipitation. This

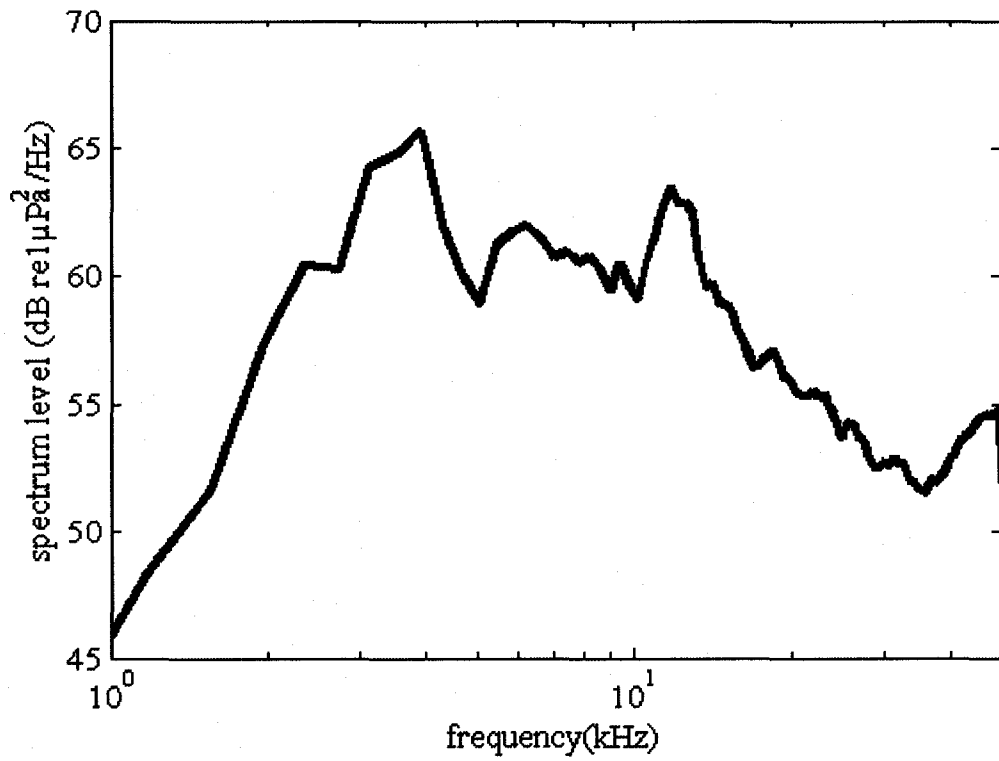


Figure 2.4. The sound spectrum generated by snow. The spectral level calculated in dB and the frequency in Hz.

data is shown in blue in Figure (2.5). In addition, the tank has four edges along the top that are 15 cm wide. When snow strikes these edges it could make a noise that contributes to the measured signal. The water surface was covered with plastic “bubble wrap” and a piece of wool fabric to test for this contamination by isolating the sound of snow striking the tank edges. Figure (2.5) shows the noise generated by snow striking the tank edges in yellow. A small rise in spectral levels was observed above the background noise. The noise levels of the background noise spectra are still 10 dB below the lowest sound level produced by snow falling (stellar flakes), and it will not affect the signal generated by falling snow.

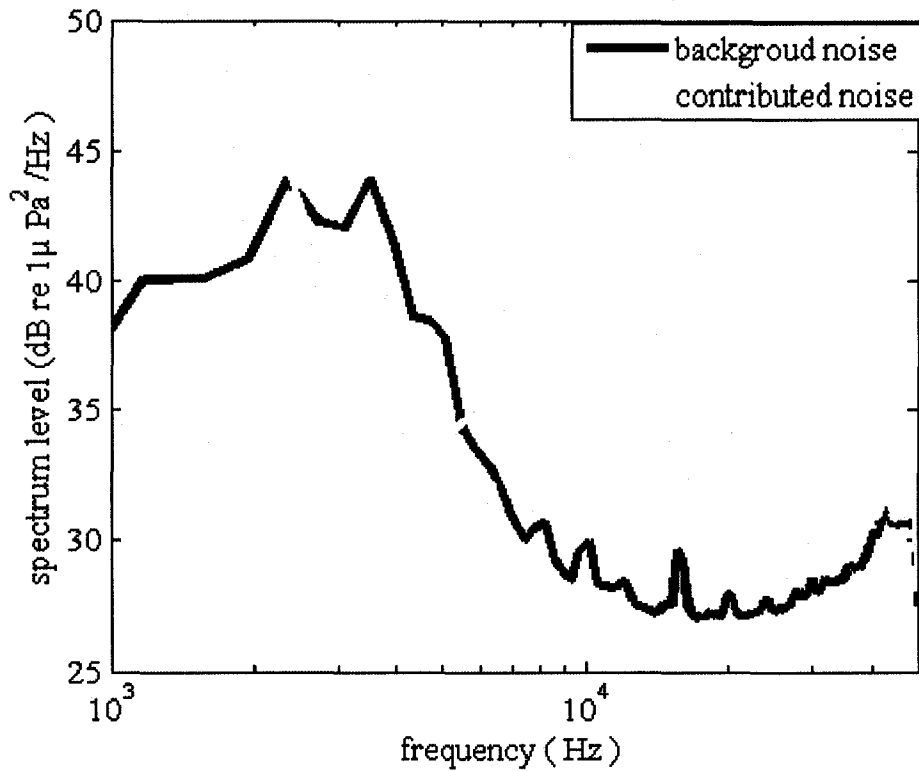


Figure 2.5. The spectral levels in dB of the background noise selected without precipitation (no snow) plotted in blue. The spectrum in yellow is recorded during a snow event but using bubble wrap and a piece of wool fabric to cover the water surface: the noise is contributed by snow striking the edges of the tank and by wind.

Chapter 3

The Results and Discussion

3.1 The Results

3.1.1 Spectra for different snowfall types

Data were collected from fourteen experiments of different snowfall events and different snowfall rates. These data sets were calibrated and analyzed using the FFT method then averaged over the whole time series of each event as described in section 2.2. Snowfall types were classified by the international classification system presented in the introduction. One other form of solid precipitation for which data were collected was Frozen rain, it's not classified as a snowfall type, but those observations are compared with the noise generated by snowfall types.

Although there are ten different types of snowflakes identified in the international classification scheme, we only had opportunity to record seven different types. The types that we didn't detect are Capped column, Ice

pellet, and Hail. Underwater sound spectrum produced by Hail is shown in Figure (1.1). Capped column would likely have the same mechanism as Column snow type in producing underwater sound signal, as they are very similar in form. Also Frozen rain and Ice pellets would probably have the same mechanism in producing underwater sound as a result of their similar form. Due to this, we expect that the spectrum produced by Ice pellets would have the same characteristic spectrum of Frozen rain, and the spectrum of Column snow types would look similar to the Capped column spectrum.

Figure (3.1) shows the power spectral density for all snow types observed as well as for Frozen rain. There are three clearly similar groups that appear in these spectra; Frozen rain with very high spectral levels, Graupel, Irregular, Needle, and Irregular with Column at intermediate levels, and finally Stellar, Spatial dendrite, and Plate which occur essentially at the background noise level.

The frozen rain spectrum has the highest spectral level that reached about 78 dB (re 1 μ Pa/Hz) with a spectrum that had no characteristic peak. Even though the snowfall rate for this event was low (5 mm/hr) compared to snowfall rate of other events (as high as 46 mm/hr). Also the gradual rise in spectral levels above 30 kHz was not clear in Frozen rain.

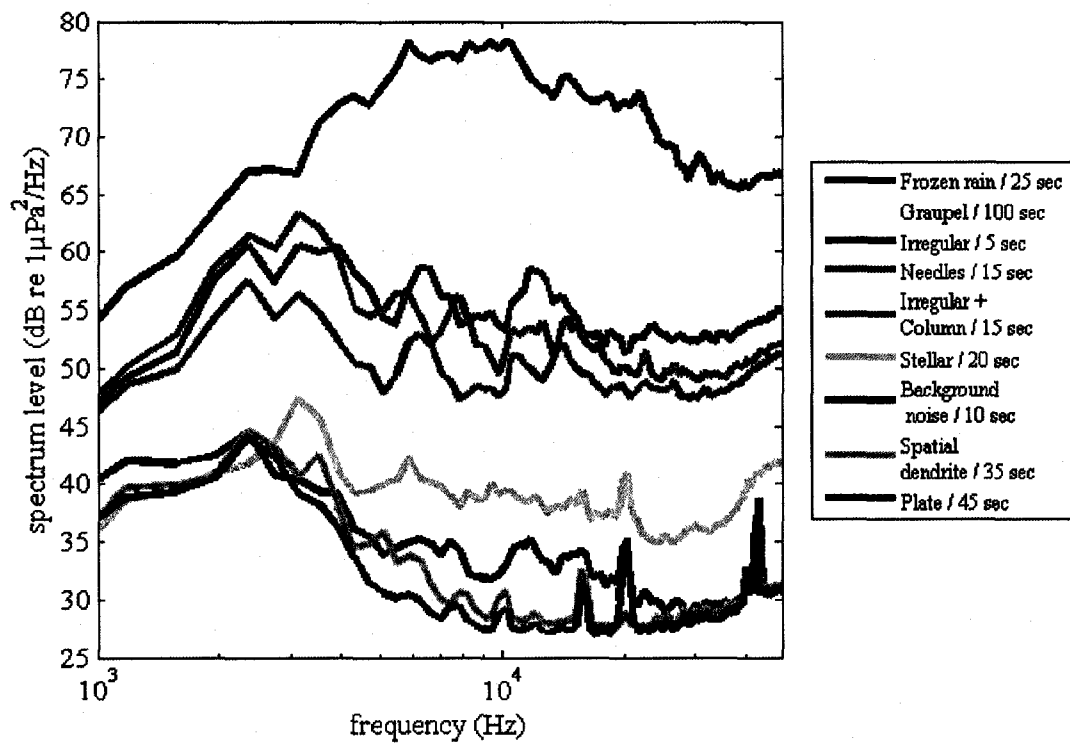


Figure 3.1. The spectral levels in dB as a function of frequency in Hz for seven types of snow crystals. Also shown is a background noise spectrum collected as it is snowing by covering the water surface. The numbers in the legend show the time in (seconds) for each data type that has been used in creating the spectrum.

In the intermediate spectral levels between 45 – 60 dB, there are four spectra that show similar spectral characteristics; below 4 kHz these spectra illustrate high levels, a gradual rise in spectral levels appears at frequency above 30 kHz, where the sound levels increases about 3 – 4 dB. Graupel and Irregular snowflakes had a characteristic spectrum with a peak at about 12 kHz, reaching a level of 60 and 57 dB (re $1\mu\text{Pa}^2/\text{Hz}$) in the spectra of Graupel and Irregular flakes respectively. The 12 kHz peak is also visible in the spectra of Needle and Irregular Column flakes but not as clearly as in the previous spectra. This peak was not recorded in any of the previous studies of snowflakes. Scrimger et al. (1987) didn't have the spectral resolution to resolve this peak, and McConnell et al. (1992) and Crum et al. (1999) don't report snowflake type. This peak is unique for these four spectra, which is expected to be a result of bubble resonance as will be discussed later in this chapter. For the rest of this study these four snow types that make the peak at 12 kHz will be referred to as “resonant flakes”.

For those lower level spectra, the Stellar flakes spectrum did show a rise in sound level above the background noise of about 5 to 8 dB without the characteristic peak at 12 kHz seen in the resonant flakes spectra.

Scrimger (1985) mentioned this slight rise in the spectral level above the background noise in the snow spectra recorded in his experiment. Spectra from Plate and Spatial dendrite flakes are shown separately in Figure (3.2) along with background noise for the instrument to magnify the characteristic of these low level spectra. There is essentially no signal as the spectra look almost exactly as the background noise without precipitation. The Plate spectrum shows a peak at a frequency of about 20 kHz, which is probably due to instrument electric noise. Also a gradual increase in sound levels appears above 30 kHz. High sound levels do occur at lower frequencies in these spectra and that signal (caused by wind) will be discussed later in section 3.1.4.

3.1.2 A comparison between rain and snow spectra

In order to observe the differences between rain and snow spectra, 15 seconds of data were collected during a period of rain that has rainfall rate of about 2 mm/hr. Figure (3.3) shows a spectrum of light rain (drizzle) along with the spectra of resonant flakes. The characteristic spectral peak associated with light rain spectrum reached to 68 dB at a frequency of about

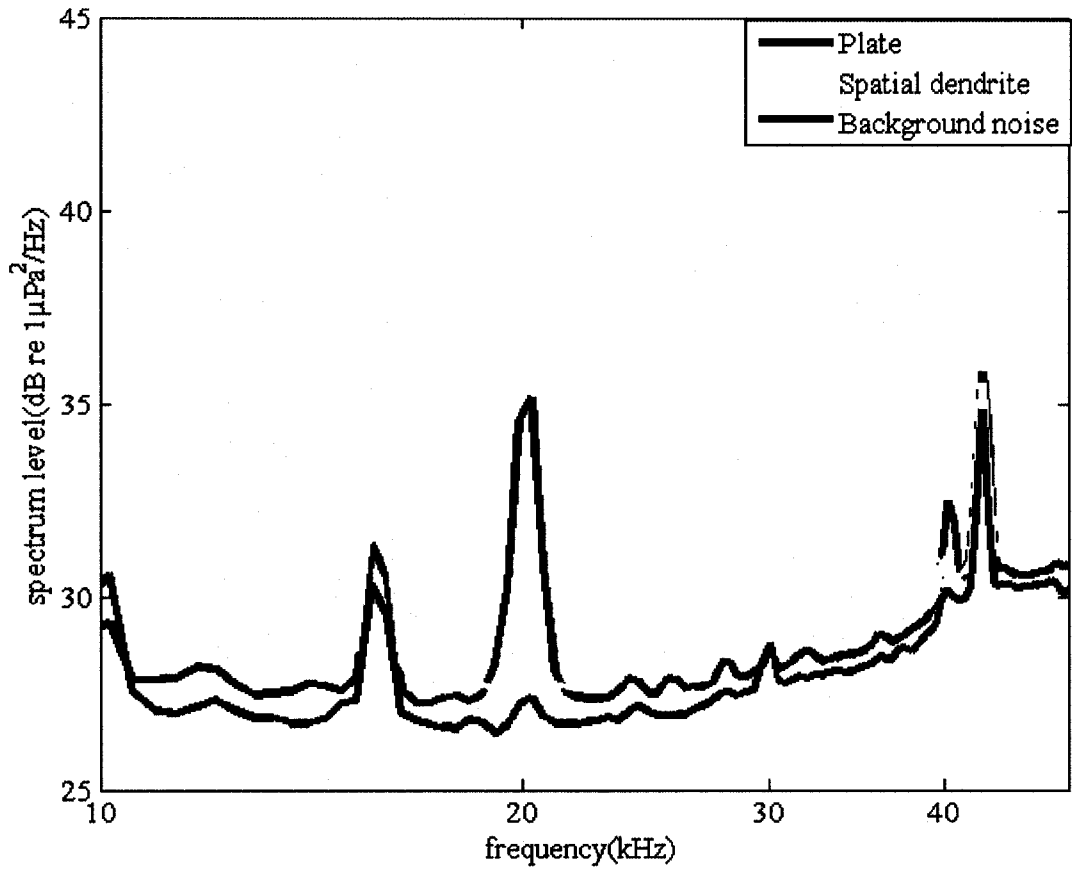


Figure 3.2. The spectral level in dB as a function of frequency in Hz for; Spatial dendrite crystals, Plate crystals, and the background noise measured when there is no precipitation.

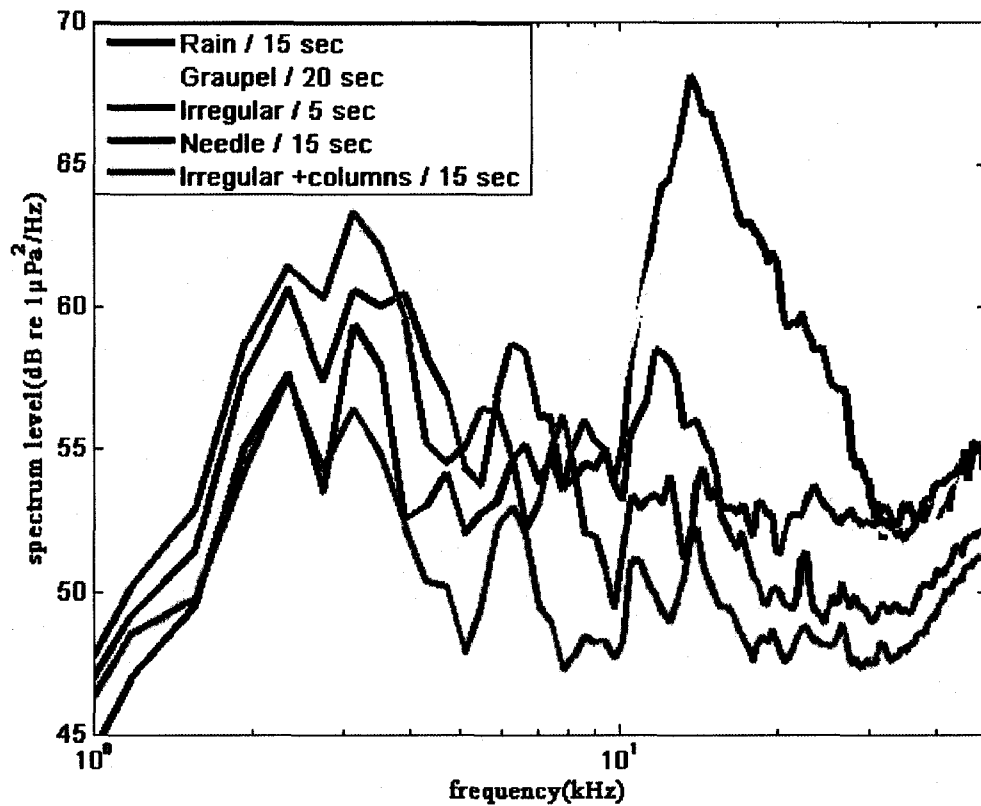


Figure 3.3. Sound spectra of different snowfall types and light rain. the snowfall spectra shows a peak at 12 kHz. The numbers in the legend indicate the time duration of the recorded snow periods.

13.7 kHz. This peak is similar in form to the peak in resonant flakes spectra at a frequency of 12 kHz. Even though snowfall rate of Graupel flakes was 46 mm /hr and for Irregular snowflakes was 24 mm/hr, the peak in the rain spectrum was much higher with a precipitation rate of only 2 mm/hr. A rise in spectral level of about 3 dB was detected at frequencies between 30 kHz and 50 kHz for the light rain spectrum similar to that seen in snow spectra.

3.1.3 The relationship between sound level and snowfall rate.

Our concern was to explore the relation between sound level and snowfall rate, to see if snowfall rates can be estimated by measuring the sound spectra generated by snow falling. Figure (3.4) shows different snow spectra sorted by snowfall rates. The highest spectrum level was the dark blue spectrum, with a high snowfall rate of 46 mm/hr for Graupel flakes. Next highest was also Graupel flakes with a snowfall rate of about 14 mm/hr, followed by Column with Irregular flakes with a snowfall rate of about 25 mm/hr. The spectrum of Needle with Frozen rain flakes reached a higher spectral level than expected compared with the other observations, given that the snowfall rate is 2 mm/hr. Another unusual spectrum in this example is that of unexpected behavior from the spectrum with snowfall rate

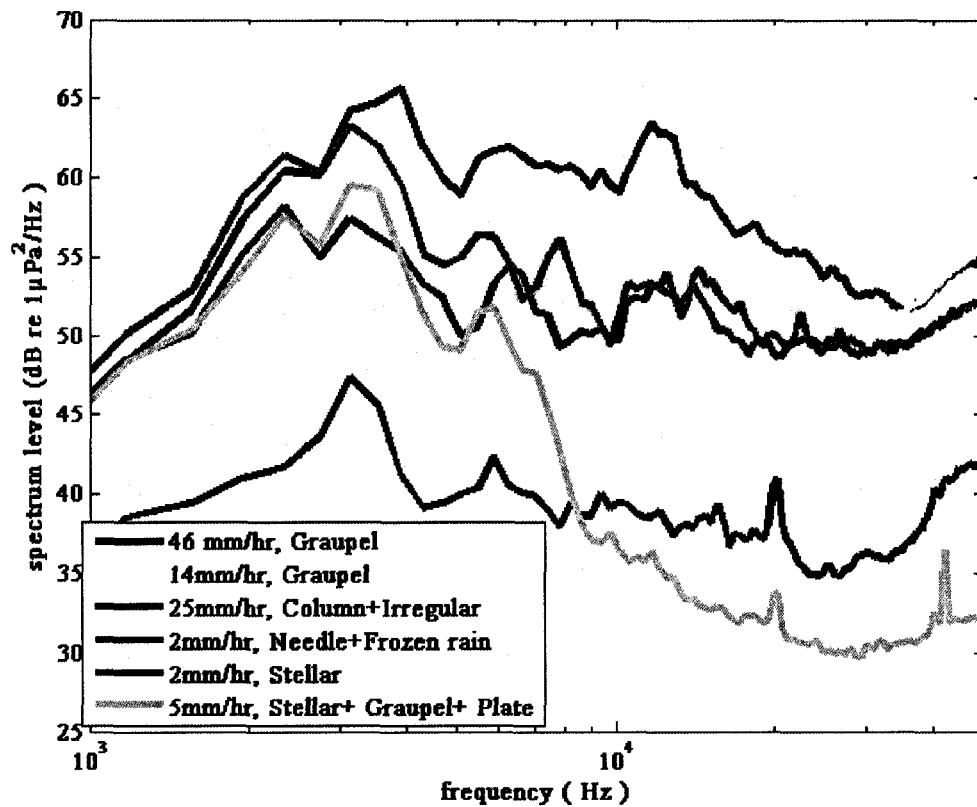


Figure 3.4. The power spectral density for different snow events with different snowfall rate, the numbers indicate the snowfall rate in mm/hr for each snowfall event.

of 5 mm/hr, which has high spectral level at frequencies below 4 kHz, and then the sound level falls down rapidly to reach the background noise level at frequencies above 4 kHz.

The sound spectra of different snowfall periods shown in Figure (3.4) show little apparent order. It is however, encouraging that the highest spectral level occurs at the highest snowfall rate of 46 mm/hr. Some of this inconsistency is a result of the changing snow type, such as the spectrum of a snowfall rate of 2 mm/hr (light blue) has a higher spectral level than would be expected due to the snow types in this event (Needle with Frozen rain flakes). The presence of Frozen rain in those observations causes the unexpected rise in spectral level for this event. The other anomalous snow spectrum is that with snowfall rate of 5 mm/hr because of its high levels at low frequencies. In this case, the spectra were dominated by wind speed effects below 4 kHz. At higher frequencies where wind is not a factor the reduced sound level is more consistent with the Stellar, Graupel, and Plate flakes that occur (Plate and Stellar flakes do not produce sound).

Clearly there is no simple correlation between overall spectral level and snowfall rate observed in this study. The spectral level depends not only on snowfall rate but also on the type of falling snow.

In order to understand the progression of spectra shown in Figure (3.1), it is necessary to consider the different frequency regions of the spectra. Low frequencies are often dominated by wind effects and so we explore that relationship, the middle frequencies (10 – 15 kHz) span the region of resonant response, and high frequency (above 30 kHz) is the region that has been identified as being unique to snow.

3.1.4 Wind speed effect at frequencies below 4 kHz

As mentioned before, high sound levels were observed in all spectra at frequencies between 2 to 4 kHz as shown in Figure (3.1), the spectral level at these frequencies do not vary sensibly with snow type or precipitation rate. For this reason a systematic relationship with wind speed was explored to determine the wind noise effects on low frequency sound. Figure (3.5) shows the averaged spectral level of frequencies between 2 – 4 kHz for the fourteen snow events detected through experiments as a function of wind speed in km/hr. These data are correlated with $R = 0.5$ (p-value = .1); a linear fit to the data gives Sound Level in dB as;

$$\text{Sound Level} = (0.7 \pm 0.4) \times \text{Wind Speed} + (38 \pm 8), \quad 3.1$$

where *Wind Speed* is in kmh.

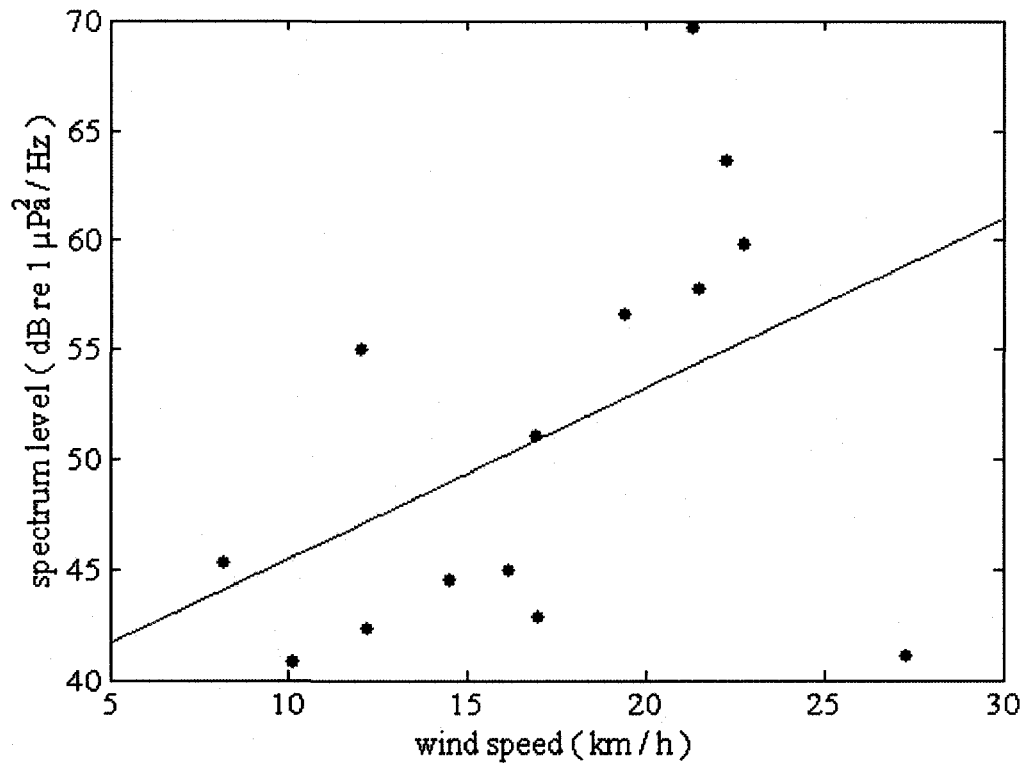


Figure 3.5. The averaged spectral level in dB of frequencies below 4 kHz with respect to wind speed in km/hr. Each point represents a single snow event. The data are correlated with $R = 0.5$ (p-value = 0.1). The line represents a linear fit to the data with a slope of (0.8 ± 0.4) dB/kmh, and an intercept of (38 ± 8) dB.

The fitted line shows that the spectral level increases as the wind speed increases. There is some variability in some of the events, as the experiment was held behind the building which suppresses the wind effect in some circumstances depending on the direction of the wind. This contributes to the high uncertainties and limited degree of correlation. The occurrence of this sound level dependency on wind speed at frequency below 4 kHz shows that correlation with snowfall rate cannot be expected at this range of frequency.

3.1.5 Snow spectra at frequencies between 10 – 15 kHz

The peak of light rain at a frequency of 13.7 kHz shown in Figure (3.3) is generated due to the damped oscillations of microbubbles produced by entraining small raindrops into the water. Crum et al. (1999) have suggested some mechanisms that could be responsible for generating underwater sound due to snow and rain which are air engulfment, frozen bubble release, and the occurrence of hollow ice crystals. These mechanisms could explain the peak that appears in some spectra of snowflake types. When resonant flakes strike the water surface, a gas bubble would be released from the inside of

ice crystals. Or the air bubbles would enter the water surface due to the impact of snowflakes with water. As soon as the gas bubbles enter the water they oscillate at a frequency of 12 kHz causing a characteristic peak at this frequency which appears in resonant flakes spectra. Both the observations of Scrimger et al. (1987) and McConnell et al. (1992) do not mention this peak in snow spectra, but this omission could be explained because the recorded underwater sound might belong to those snow types that don't have the peak of the resonant flakes. As mentioned in chapter one, Crum et al. (1999) show that snowflakes and raindrops have the same damping constant of the resonance gas bubbles. Also the spectral peak arising between 13 – 15 kHz is caused by bubble resonance (Laville et al., 1990). This indicates that a peak should be present in the spectra of snow that create underwater sound due to the bubble resonance mechanism. The snowfall rate observed for Graupel and Irregular (46 and 24 mm/hr respectively) were much higher than the observed rainfall rate (≈ 2 mm/hr). Despite this difference, the peak of the light rain spectrum reaches to 68 dB compared to the peaks of 61 and 58 dB seen in the spectra of Graupel and Irregular flakes respectively. This indicates that snow generates less sound than light rain spectrum in the region of this damped oscillation peak.

To detect if there is a relation between snowfall rate and spectral level at 12 kHz, we inspected this relation in Figure (3.6), which shows the averaged spectral level at frequencies between 10 – 15 kHz with respect to snowfall rate of the resonant flakes spectra. The linear fit shown in the figure has a slope of (0.22 ± 0.07) dB/(mm/hr), and intercept (49 ± 2) dB and indicates that there is a correlation ($R = 0.9$, $p\text{-value} = 0.09$) between snowfall rate and sound level at frequencies between 10 – 15 kHz for those resonant flake types. The limited amount of data available requires that this correlation be confirmed by more experiments in the future, particularly on snow types that generate the characteristic peak at 12 kHz.

3.1.6 Snow spectra at frequencies above 30 kHz

A very important observation is that light rain and snow spectra have a similar rise in the spectral level of about 3 dB at frequencies above 30 kHz. This was observed in several studies as the only contribution of underwater sound produced by falling snow, and is documented as appearing only in snow spectra. Figure (3.3) shows a remarkable similarity for this rise above 30 kHz in both light rain and snow type spectra.

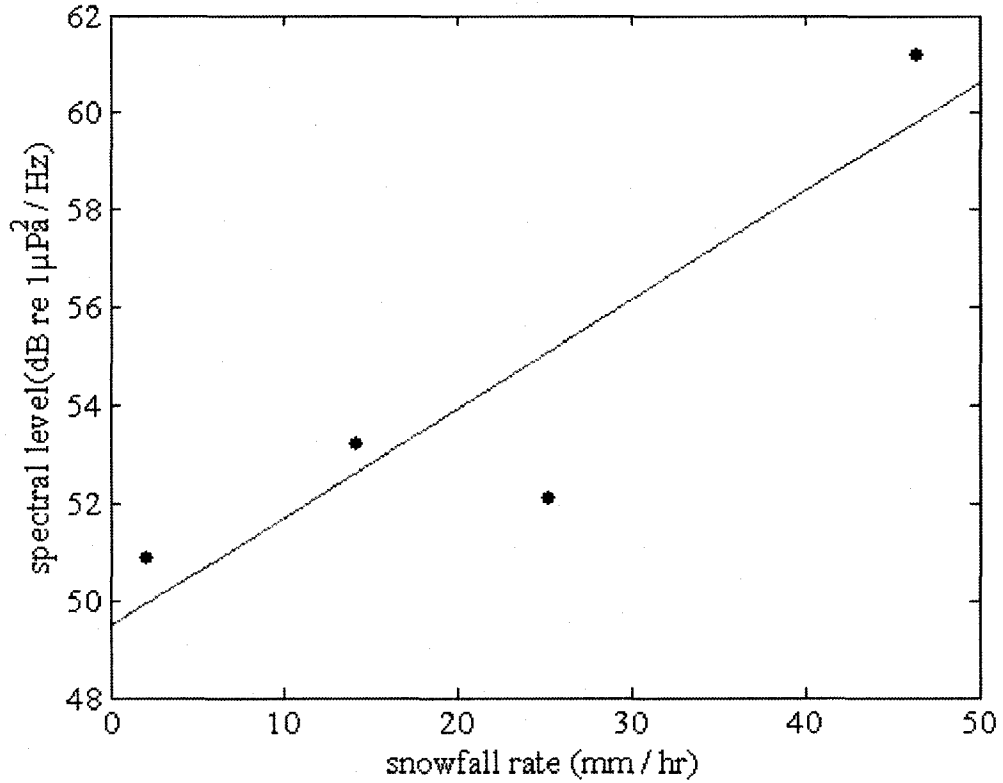


Figure 3.6. The averaged spectrum level in dB of frequencies between 10 – 15 kHz with respect to snowfall rate in mm/hr for the previous snowfall events plotted in figure (3.4). The data points indicate the snow spectra that have a peak at frequency of 12 kHz. The line represents the linear fit for the data points with a slope (0.22 ± 0.07) dB/(mm/hr), and intercept (49.4 ± 2.0) dB.

The high frequency end of the spectrum is very sensitive to the presence of bubbles in the water. High wind speed (above 10 m/s) or extremely heavy rainfall rate or both creates a bubble layer directly under the water surface. This layer could attenuate the sound generated by rain and absorb the signal above 10 kHz causing a rapid decrease in the spectral level above that frequency (Nystuen et al., 1993, Nystuen et al., 2001, Nystuen, 1986, Ma and Nystuen, 2005). The surface layer of ocean, seas, or lakes is full of bubbles created due to several factors such as breaking waves, marine life, and gas exchange. This layer can mask the high frequency signal, which might be the reason why other field studies did not detect the rise of noise level above 30 kHz in light rain spectra measured in field experiments. Such bubbles do not collect in the experimental tank used here because of the use of fresh water and the absence of wave action.

Figure (3.7) shows the relationship between the averaged snow spectra at frequencies above 30 kHz with snowfall rate for the spectra that show a rise above 30 kHz in order to explore if there is a relation between the spectral levels above frequency of 30 kHz and snowfall rate. These data

are poorly correlated ($R = 0.7$, $p\text{-value} = 0.3$). A linear fit shown in figure 3.7 gives a slope of (0.2 ± 0.3) dB/(mm/hr): the high uncertainty in the slope

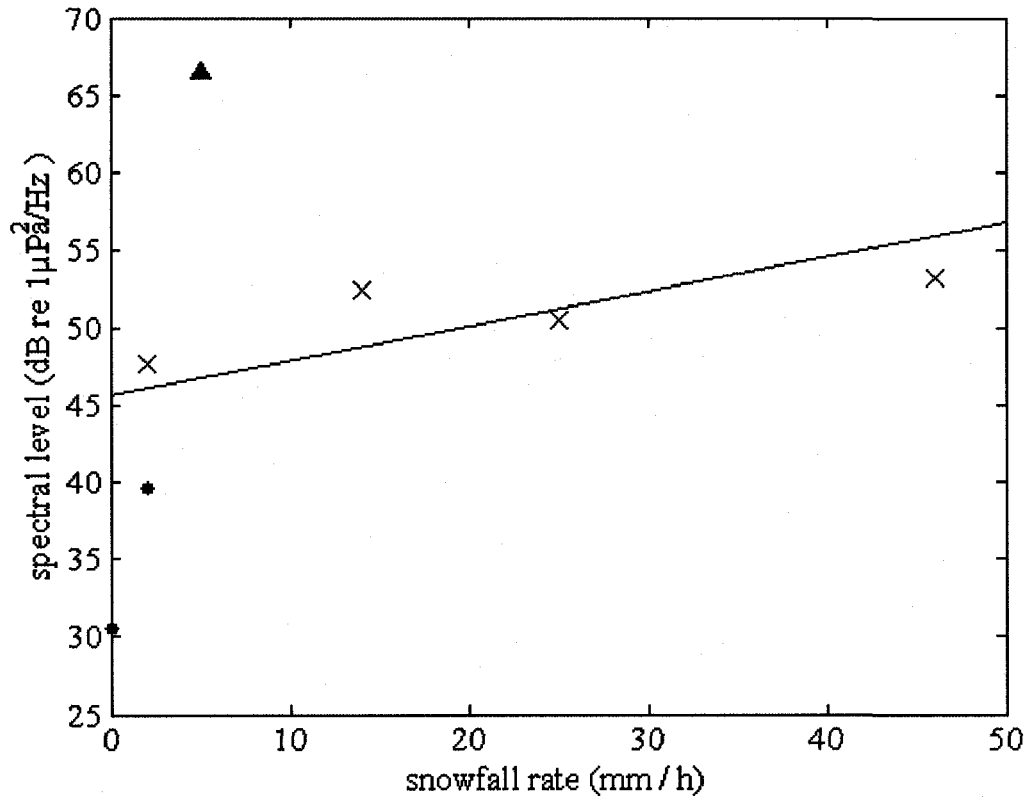


Figure 3.7. The averaged spectrum level in dB for frequencies above 30 kHz with snowfall rate of the snow events plotted in Figure (3.1). The points (x) indicate the resonant flakes, (•) for the spectra which do not create underwater sound (Spatial dentrite, Stellar, Plate), (▲) for the Frozen rain spectrum. The resonant flake data have a correlation of 0.7 (with p-value of

0.3). The line represents the linear fit for the resonant flake data with a slope (0.2 ± 0.3) dB/(mm/hr), and intercept (46 ± 6) dB.

is a result of the poor correlation between the snowfall rate and snow spectra at frequencies above 30 kHz.

3.2 Discussion

The main aims in this study which are mentioned in the introduction is to calculate the spectrum of each snow type, to discriminate the snowflake types that generate underwater sound, and to find the relationship between the spectral level and snowfall rate.

3.2.1. Different snowflake types produce different snow spectra

The seven snow types observed along with the Frozen rain spectra could be sorted into three different groups. The first group is Frozen rain that likely appears as accumulation of frozen raindrops generates the highest sound level. Although it was not the highest precipitation rate, this sound

level exceeded by about 12 dB the sound level of the highest snow spectra; Frozen rainfall rate was about 5 mm/hr while the highest snowfall rate reached to more than 46 mm/hr. The second group are the resonant flakes that produce a characteristic peak at a frequency of 12 kHz. This peak is generated due to the resonant bubbles that enter the water as a result of the impact or the release of the frozen air bubble inside the crystal. The last and quietest group is the Stellar flakes, a slight rise in the background noise was observed without showing any characteristic spectral peak as in the previous types. Plate and Spatial dendrite flakes produce no discernable sound above that of the background noise spectrum.

A quick look at the forms of snow types in the international classification system shown in Figure (1.6) carries out an idea about snow forms that are noisy and the forms that are quiet. The resonant flakes that generate sound with a peak at 12 kHz are Graupel, Irregular, Column, and Needle. A close look at their forms shows that these types have three dimensional shapes. While the types that are quiet are Plate, Stellar, and Spatial dendrite. Stellar and Plate crystals have flat shapes that possibly do not transfer enough momentum into the water as they strike the water surface. In contrast, the Spatial dendrite crystals observed in the experiment

were large crystals with structure in many different planes, but they do not generate sound. The snowfall rate of this particular event was very low (less than 1 mm/hr), so it is possible that the Spatial dendrite flakes didn't produce sound due to the low snowfall rate. Additional experiments need to be done on that particular snow type. The other snow types detected in the experiment agree with the idea that flat and thin snow crystals are quiet and the three dimensional snow crystals are noisy.

Because of the weak impact of snowfall with water and the little potential transferred into the water due to the impact; a comparison was done between the resonant snow types and light rain (drizzle) rather than heavy rainfall. This comparison showed similar peaks appeared in both light rain and the resonant flakes at 13.7 kHz and 12 kHz respectively, with much higher sound level for the light rain which suggests that light rain has more momentum which can produce bubbles as a result of the impact. Crum et al. (1999) suggest that only about 10% of snowflakes made any noise.

The rise in spectral level above 30 kHz can be observed in light rain as well as in all detected snow types, which makes this property not exclusive for snow spectra only. This is likely explained through the behavior of the bubble layer generated under the water surface which will

absorb the high frequency sound above 30 kHz when the sound is recorded in open seas, oceans or lakes. This layer of bubbles was not created in the test tank, because of that the high frequency rise in sound level is detected in rain and snow spectra. The gradual rise in sound level of snow spectra is not exclusive to snow and it also appear on light rain, and it can not be an indication of snowfall events.

To see if there is a correlation between snowfall rate and sound levels, we examined the relation at different frequency ranges of snow spectra. At frequencies below 4 kHz the sound levels demonstrate a correlation with the wind speed; as the wind speed increases the sound level increases. In the frequency range between 10 – 15 kHz where the resonant flakes generate a peak, only four events were observed but this limited data does suggest a correlation and linear sound level response exists (Figure 3.6). At frequency above 30 kHz Figure (3.7) doesn't show a clear relationship between snowfall rate and the averaged sound level. Again, because of the limited amount of data more studies are needed to be done to explore the relationship between snowfall rate and snow spectral levels.

3.2.2 Snowfall rate measurements

In addition to the uncertainty in any method used to measure snowfall rate, some problems in comparing sound levels to precipitation rates could occur because of the inconsistencies in the snowfall rate measurements. In order to assess the reliability of the optical rain gauge OWI-430 being used, the measured snowfall rate using the rain gauge was compared with the snowfall rate recorded by radar imagery. Figure (3.8) shows this comparison, where snowfall rate measured by the rain gauge is plotted with respect to snowfall rate recorded by Environment Canada. The data are significantly correlated ($R = 0.8$, $p\text{-value} = 1 \times 10^{-6}$) a linear fit gives a slope of (1.8 ± 0.2) demonstrating a clear agreement, although very heavy snowfall rates show substantial variability. It should be mentioned that snowfall rate measurements using the rain gauge could be affected by the building where the experiments were held. The turbulence caused due to the building could change the snowfall rate from location where the experiments were held and the place where the rain gauge was mounted on top of the building. Also wind direction interactions with the building will cause changes in the snowfall distribution at the site of the experiment.

The correlation method used to compare snowfall rate measurements using rain gauge and radar imaginary also has a sampling difference, the rain gauge calculates point measurements of snowfall rate at the exact location, where these measurements are recorded every minute. While snowfall measurements by radar imaginary are averaged over a large area and recorded every ten minutes.

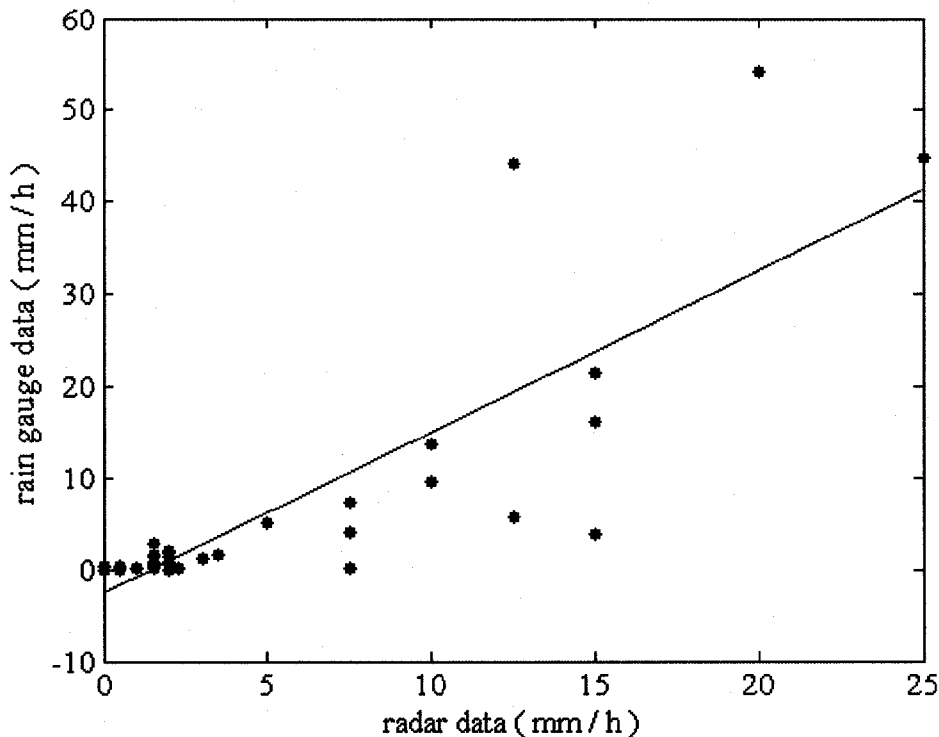


Figure 3.8. A comparison between rain gauge data and radar data in mm/hr. The line represents the linear fit for the data results with a slope (1.8 ± 0.2), and intercept (-2.6 ± 1.6) dB.

Chapter 4

Summary and Conclusions

Measuring underwater sound at sea is expensive and complicated. A variety of noise sources such as from shipping, wind or biological origin can contaminate the data. Also, accurate simultaneous weather observations can be difficult to obtain. In this study, sounds generated by snowflakes falling on water have been observed using a small (80 × 60 × 60) cm test tank.

Several experiments were held in winter 2007 in St. John's, Newfoundland outside the Chemistry-Physics building. Seven snow types were detected in a variety of weather conditions (Plate, Spatial dendrite, Stellar, Irregular, Column, Needle, and Graupel) in addition to Frozen rain. Wind speeds were measured using a roof – top weather

station on the MUN Chemistry-Physics building and snowfall rates were measured by an OWI-430 rain gauge also mounted on the same building. Snowfall rate was compared to and agrees with the data recorded by the Holyrood weather radar image taken from the Environment Canada Web Site.

The goals of this study have been to create a spectrum for each snow type that generates underwater sound, and to compare between the spectrum of rain and snow. Data has also been used to explore the relation between snowfall rate and sound level.

In this study we observed that different snow types have different underwater sound spectra. The Frozen rain sound spectrum shows high sound levels with no characteristic peak. The resonant flakes (Graupel, Irregular, Column, and Needle) generate spectra with a peak at a frequency of 12 kHz. And Stellar, Plate and Spatial dendrite flakes produce no sound. It would appear that flat snow crystals are quiet, while three-dimensional snow crystals generate sound.

Rain and resonant flakes were observed to generate a peak at frequency between 12 – 13.7 kHz with behavior consistent with that of

bubble resonance as reported by Crum et al. (1999).

The relation between snowfall rate and sound level is not determined in this study as sound level depends on snowfall rate and snow type. Given this complication the data is not enough to demonstrate the relation. The analysis does show that there is a possible relation between snowfall rate and sound level at frequencies between 10 – 15 kHz and 30 – 50 kHz. The possibility of measuring snowfall rate using underwater sound produced by snow is a promising technique but measuring the relationship between the snowfall rate and snow spectral level needs more studies to be explored.

The sound level below 4 kHz showed a correlation with wind speed in this study; as the wind speed increased so did the sound level. Lower frequency sound in the ocean is known to be affected by wind speed (McConnell et al., 1992), but the contamination in the present observations makes exploration of this spectral region impossible. A peak appeared at a frequency of 12 kHz in the resonant flakes spectra which is not detected in any other studies.

Previous studies have identified a rise in spectral level at frequencies above 30 kHz as a characteristic of snowfall (Scrimger et al., 1987, McConnell et al., 1992). The present observations are consistent with that observation but it is also seen in rainfall spectra. What is likely occurring is that precipitation in general causes an increase in high frequency sound levels. However, rain probably injects more air bubbles deeper into the water surface and these bubbles quench that high frequency sound (Nystuen, 2001). If this were the case, any wave breaking activity would also act to suppress the high frequency signal of both rain and snow.

4.1 Future work

These are some suggestions for future work:

- It will be useful to explore underwater sound produced by snow using additional field experiments and compare it with the results we have in this study.
- We suggest adding high speed movies to track the event of falling snowflakes on water surface and explore the mechanism that generates sound by falling different types of snowflakes on water.

- We didn't have the chance to track the ice pellet and Capped column snow types.

Bibliography

- 1) Lawrence A. Crum, Hugh C. Pumphrey, Ronald A. Roy, and Andrea Prosperetti. *The underwater sound produced by impacting snowflakes*. J. Acoust. Soc. Am. 106 (4), 1765 – 1770, 1999.
- 2) D. M. Farmer and S. Vagle. *On the determination of breaking surface wave distribution using ambient sound*. J. Geophys. Res., 93, 3591 – 3600, 1988.
- 3) Peter V. Hobbs. *Ice Physics*. Clarendon Press. Oxford. 1974.
- 4) <http://www.agiudetosnowflake> .
- 5) <http://www.weatheroffice.gc.ca/radar> .
- 6) V. O. Knudsen, R. S. Alford, and J. W. Emling. *Underwater ambient sound*. J. Mar. Res. 1, 410 – 429, 1948.

- 7) Edward R. LaChapelle. *Field Guide to Snow Crystals*. J. J Douglas Ltd. Vancouver, 1969.
- 8) Frederic Laville, Grayson D. Abbott, and Matthew J. Miller. *Underwater sound generation by rainfall*. J. Acoust. Soc. Am. 89 (2), 715 – 721, 1991.
- 9) Barry B. Ma, Jeffrey A. Nystuen. *Passive Acoustic Detection and Measurement of Rainfall at Sea*. American Meteorological Society, 22 (8), 1225 – 1248, 2005.
- 10) Barry B. Ma, Jeffrey A. Nystuen, and Ren-Chieh Lien. *Prediction of underwater sound levels from rain and wind*. J. Acoust. Soc. Am. 117 (6), 3555 – 3565, 2005.
- 11) C. Magono and C.W. Lee. *Meteorological classification of natural snow crystals*. J. Fac. Sci., Hokkaido Univ., Series VII, 2, 321-362.
- 12) Steven O. McConnell, Michael P. Schilt, and J. George Dworski. *Ambient noise measurements from 100 Hz to 80 kHz in an Alaskan fjord*. J. Acoust. Soc. Am. 91 (4), 1990 – 2003, 1992.

- 13) Herman Medwin, Mathew M. Beaky. *Bubbles sources of the Knudsen sea noise spectra*. J. Acoust. Soc. Am. 86 (3), 1124 – 1130, 1989.
- 14) Herman Medwin, Jeffrey A. Nystuen, Peter W. Jacobus, Leo H. Ostwald, and David E. Snyder. *The anatomy of underwater rain noise*. J. Acoust. Soc. Am. 92 (3), 1613 – 1623, 1992.
- 15) Herman Medwin and Clarence S. Clay. *Fundamentals of Acoustical Oceanography*. Academic Press, USA, 1998.
- 16) W. K. Melville, M. Loewen, F. C. Felizardo, A. Jessup, and M. J. Buckingham. *Acoustic and microwave signature of breaking waves*. Nature, 336, 54 – 59, 1988.
- 17) U. Nakaya. *Snow Crystals: Natural and Artificial*. Harvard University Press, 510 pp.
- 18) Jeffrey A. Nystuen. *Rainfall measurements using underwater ambient noise*. J. Acoust. Soc. Am. 79 (4), 972 – 982, 1986.
- 19) Jeffrey A. Nystuen, Charles C. McGothin, and Michael S. Cook. *The underwater sound generated by heavy rainfall*. J. Acoust. Soc. Am. 93 (6), 3169 – 3177, 1993.

- 20) Jeffrey A. Nystuen, Harry D. Selsor. *Weather Classification Using Passive Acoustic Drifters*. Journal of Atmospheric and Oceanic Technology. 14, 656 – 666, 1997.
- 21) Jeffrey A. Nystuen. *Listening to Raindrops from Underwater: An Acoustic Disdrometer*. J. of Atmospheric and Oceanic Technology. 18, 1640 – 1657. 2001.
- 22) Joseph A. Scrimger. *Underwater noise caused by precipitation*. Nature. 318, 647 – 649, 1985.
- 23) Joseph A. Scrimger, Donald J. Evans, Gordon A. McBean, David M. Farmer, and Bryan R. Kerman. *Underwater noise due to rain, hail, and snow*. J. Acoust. Soc. Am. 81 (1), 79 – 86, 1987.
- 24) H.P. Press, B.P. Flannery, S.A. Teukolsky, W.T. Vetterling. *Numerical Recipes: The Art of Scientific Computing*. Cambridge University Press, 818 pp., 1986.
- 25) Svein Vagle, William G. Large, and David M. Farmer. *An Evaluation of the WOTAN Technique of Inferring Oceanic Winds from Underwater Ambient Sound*. Journal of Atmospheric and Oceanic Technology, 7, 576 – 595, 1990.

- 26) William T. Vetterling, Saul A. Teukolsky, William H. Press, and Brian P. Flannery. *Numerical Recipes: the art of scientific computing*. Cambridge University Press, New York, 1989.
- 27) Gordon M. Wenz. *Acoustic Ambient Noise in the Ocean: Spectra and Sources*. J. Acoust. Soc. Am. 34 (12), 1936 – 1956, 1962.

APPENDIX A.

Spectral analysis and Fourier transform.

In these experiments it is important to calculate the power contained in the signal within the frequency domain, calculating the power spectral density would be the ideal method to deal with and infer these data. In this section we will describe the functions used in analyzing our data. Fourier transform equations can represent the same function in the frequency domain and the time domain as follows (Press *et al.*, 1986).

$$H(f) = \int_{-\infty}^{\infty} h(t)e^{2\pi i f t} dt \quad (1)$$

$$h(t) = \int_{-\infty}^{\infty} H(f)e^{-2\pi i f t} df \quad (2)$$

Where $H(f)$ is the amplitude as a function of frequency, and $h(t)$ represent the same function in the time domain. Time is measured in seconds and the frequency f in cycles / second (hertz). Some of Fourier transforms properties

made work easier and its worth to mention these properties in general. First it is a linear process that is Fourier transform of the sum of two functions equal the sum of Fourier transform of each function. Second is the Convolution theorem define that Fourier transform of the convolution of the two functions ($g * h$) is equal to the product of their individual Fourier transforms.

$$g * h = \int_{-\infty}^{\infty} g(\tau)h(t - \tau)d\tau = \int_{-\infty}^{\infty} h(\tau)g(t - \tau)d\tau \quad (3)$$

$$g * h \Leftrightarrow G(f)H(f), \quad (4)$$

Where $h(t)$, $g(t)$ are two different functions, and $H(f)$, $G(f)$ are their Fourier transform respectively. This expresses the amount of overlap of one function $h(t)$ as it is shifted over another function. Finally the Parseval's theorem which means that the total power in a signal is conserved, and can be computed either in the time domain or in the frequency domain by this formula

$$\text{Total Power} \equiv \int_{-\infty}^{\infty} |h(t)|^2 dt = \int_{-\infty}^{\infty} |H(f)|^2 df \quad (5)$$

In the experiment, we don't deal with continuous functions; the data is collected with discrete periodic samples where the time interval between two consecutive samples is called the sampling rate Δ . So the sampled values are

$$H_n = h(n\Delta), \quad n = \dots, -3, -2, -1, 0, 1, 2, 3, \dots \quad (6)$$

There is an important frequency called the Nyquist critical frequency f_c , which is defined as half the sampling frequency of a discrete signal processing system (in our case it's 50 kHz), given by

$$f_c = \frac{1}{2\Delta}, \quad (7)$$

The importance of Nyquist frequency in the experiment comes from the fact that if a continuous function is not band-width limited to less than the Nyquist frequency, then the power in the signal which lies outside the frequency range (f_c, f_c) will move into this range. This phenomenon is called aliasing, which contaminates the original signal and makes it difficult to recreate from the sampled signal. To avoid the aliasing problem in the experiment we can take the following steps:

1. Analog filtering of the original signal, so we use the preamplifier to filter the original data with low pass filter 50 kHz ($f > f_c$) and high pass filter 500 Hz.
2. Make sure that we use rapid sampling rate to give two points per cycle of the highest frequency component. In the experiment the sampling rate was 100 000 sample / second.

2.2.3 Discrete Fourier transform

For N successive sampled values

$$h_k \equiv h(t_k) \quad t_k = k\Delta, \quad k = 0, 1, 2, \dots, N-1 \quad \dots (8)$$

We can't pick up $H(f)$ at all values, but we can find it at distinct values

$$f_n \equiv \frac{n}{N\Delta}, \quad n = -\frac{N}{2}, \dots, \frac{N}{2} \quad \dots (9)$$

And the discrete Fourier transform of N points is

$$H_n \equiv \sum_{k=0}^{N-1} h_k e^{2ikn/N} \quad \dots (10)$$

Because the data is discretely sampled we use the fast Fourier transform algorithm, a discrete Fourier algorithm that reduces the number of computations needed for N points from $2N^2$ to $2N\log_2N$, so it is fast and more efficient. So the periodogram estimate of the power spectrum over

$\frac{N}{2} + 1$ frequencies is

$$P(0) = P(f_0) = \frac{1}{N^2} |C_0|^2, \quad (11)$$

$$P(f_k) = \frac{1}{N^2} [|C_k|^2 + |C_{N-k}|^2], \quad k = 1, 2, \dots, \left(\frac{N}{2} - 1\right) \quad (12)$$

$$P(f_c) = P(f_{N/2}) = \frac{1}{N^2} |C_{N/2}|^2, \quad (13)$$

Where

$$f_k \equiv \frac{k}{N\Delta} = 2f_c \frac{k}{N} \quad k = 0, 1, \dots, \frac{N}{2} \quad (14)$$

$P(f_k)$ represents the average of $P(f)$ over a very thin windowing function centered on f_k , the frequency offset as a function of s which related to periodogram estimates is

$$W(s) = \frac{1}{N^2} \left[\frac{\sin(\pi s)}{\sin(\pi s / N)} \right]^2, \quad (15)$$

$W(s)$ oscillates and falls off slowly when $W(s) \approx (\pi s)^{-2}$ which causes a so called “leakage” of energy between samples in the periodogram estimates. This problem can be reduced by data windowing, by multiplying the input data with a window function w_j so it makes the data change slowly from zero to its maximum. In the experiment we use the Welch window which is identified as

$$w_j = 1 - \left(\frac{j - \frac{1}{2}(N-1)}{\frac{1}{2}(N+1)} \right)^2, \quad (16)$$

The FFT length is the number of data points on which to perform the FFT. If the FFT length exceeds the size of the input data, then the data is zero padded. While if the FFT length is less than the input data, then the data truncated as needed. Also FFT length is chosen as a power of 2, such as 128, 256, 512, 1024, and 2048. In the experiments an FFT length of 256 was used. It is important to note that an increase of the number of sampled points by sampling for a longer time or using higher sampling rate will not increase

the accuracy of the periodogram estimate. That is the accuracy doesn't depend on N . Sampling for a longer time of data with a fixed sampling rate, leaves the Nyquist frequency unchanged but refines the frequency resolution within the Nyquist frequency interval. While if we sample the data with a faster sampling frequency, the frequency resolution remains the same, and the Nyquist frequency range extends to higher frequency. Now in order to reduce the variance of the estimates, there are two possible approaches:

1. Compute the periodogram estimates with finer discrete frequencies, and then make a summation over them to get one smoothed estimate.
2. Divide the original sampled data into k segments, compute the periodogram estimate for each, and then average them at each frequency.



